© 2023. Published by The Company of Biologists Ltd | Development (2023) 150, dev201026. doi:10.1242/dev.201026

RESEARCH ARTICLE

Hox11-expressing interstitial cells contribute to adult skeletal muscle at homeostasis

Corey G. K. Flynn[1], Paul R. Van Ginkel[1], Katharine A. Hubert[1,2], Qingyuan Guo[1,3], Steven M. Hrycaj[4], Aubrey E. McDermott[1], Angelo Madruga[1], Anna P. Miller[1] and Deneen M. Wellik[1,*]

ABSTRACT

Interstitial stromal cells play critical roles in muscle development, regeneration and repair and we have previously reported that *Hoxa11* and *Hoxd11* are expressed in the interstitial cells of muscles attached to the zeugopod, and are crucial for the proper embryonic patterning of these muscles. Hoxa11eGFP expression continues in a subset of muscle interstitial cells through adult stages. The induction of *Hoxa11-CreERT2*-mediated lineage reporting (Hoxa11iTom) at adult stages in mouse results in lineage induction only in the interstitial cells. However, Hoxa11iTom$^+$ cells progressively contribute to muscle fibers at subsequent stages. The contribution to myofibers exceeds parallel *Pax7-CreERT2*-mediated lineage labeling. Nuclear-specific lineage labeling demonstrates that Hoxa11-expressing interstitial cells contribute nuclear contents to myofibers. Crucially, at no point after Hoxa11iTom induction are satellite cells lineage labeled. When examined *in vitro*, isolated Hoxa11iTom$^+$ interstitial cells are not capable of forming myotubes, but Hoxa11iTom$^+$ cells can contribute to differentiating myotubes, supporting Hox-expressing interstitial cells as a new population of muscle progenitors, but not stem cells. This work adds to a small but growing body of evidence that supports a satellite cell-independent source of muscle tissue *in vivo*.

KEY WORDS: Skeletal muscle, Muscle interstitial cells, Hox genes

INTRODUCTION

Roles for Hox genes in the embryonic development of the skeletal system are well established, with loss-of-function of Hox paralog groups leading to dramatic homeotic transformations of the axial vertebrae and perturbed morphogenesis of the limb skeleton. In limb skeletal patterning, Hox paralog groups *Hox9-Hox13* have region-specific function, and loss of *Hoxa11* and *Hoxd11* gene function results in dramatic mis-patterning of the radius and ulna (Davis and Capecchi, 1996; Fromental-Ramain et al., 1996a,b; Wellik and Capecchi, 2003). In compound Hox11 mutants, in which three of the four *Hoxa11* and *Hoxd11* alleles are absent, no skeletal phenotype results, but patterning of the zeugopod-attached muscles and tendons is disrupted, supporting a direct role for Hox11 genes in muscle patterning (Swinehart et al., 2013).

Hoxa11 gene expression initiates broadly in the lateral plate mesoderm of early developing limb buds, but expression quickly localizes to the zeugopod region as it forms, and can be observed throughout development in the stromal cells surrounding the developing zeugopod cartilage and bone, in the tendons, and in a continuous population of connective tissue/interstitial stroma surrounding the zeugopod-attached myofibers (Swinehart et al., 2013). In this report, we show that Hoxa11eGFP expression in zeugopod-attached muscle interstitial cells continues through postnatal and adult life.

Limb skeletal muscle progenitors derive from the embryonic somites where muscle precursors are marked by expression of Pax3 and, later in development, Pax7 (Chal and Pourquié, 2017; Sefton and Kardon, 2019). Pax3$^+$ progenitors delaminate from the somites and migrate to the limb bud. These precursors undergo additional steps of myogenesis to generate multinucleated myocytes (Chal and Pourquié, 2017; Nassari et al., 2017; Sefton and Kardon, 2019). After maturation, muscles retain significant plasticity with the ability to undergo hypertrophy with increased use and to repair in response to injury. Repair of skeletal muscle is known to rely on satellite cells: stem cells set aside inside of the basal lamina of multinucleate muscle fibers that are self-renewing and characterized by the expression of Pax7 (Chal and Pourquié, 2017; Lepper and Fan, 2010; Lepper et al., 2011; Pawlikowski et al., 2015; Yin et al., 2013). Ablation of Pax7-expressing satellite cells leads to a profound deficit in the ability of skeletal muscle to regenerate in response to injury (Lepper et al., 2011; Sambasivan et al., 2011). Pax7-mediated lineage studies have demonstrated that satellite cells can contribute to adult skeletal muscles at homeostasis. However, ablation of satellite cells at adult stages, in the absence of injury, does not lead to early sarcopenia. Although some groups have reported that skeletal muscle remains capable of hypertrophy after ablation of satellite cells (Fry et al., 2015; Jackson et al., 2012; Keefe et al., 2015; McCarthy et al., 2011), other groups have reported that depletion of satellite cells does inhibit muscle hypertrophy (Egner et al., 2016; Goh and Millay, 2017).

A heterogenous population of stromal cells, called interstitial cells, lies outside and surrounds the basal lamina of muscle fibers. Interstitial cells are crucial for embryonic muscle patterning; neither somite-derived muscle progenitors nor satellite cells possess intrinsic muscle patterning information (Aoyama and Asamoto, 1988; Duprez, 2002; Lance-Jones, 1988; Mathew et al., 2011; Michaud et al., 1997; Nassari et al., 2017). Multiple sub-populations of interstitial cells have been defined, including pericytes, PW1$^+$/Pax7$^-$ interstitial progenitor cells (IPCs), fibroblasts, fibroadipogenic progenitors (FAPs), and smooth muscle-mesenchymal cells (SMMCs) (Giordani et al., 2019; Malecova and Puri, 2012; Mathew et al., 2011; Mierzejewski et al., 2020a; Tedesco et al.,

[1]Department of Cell and Regenerative Biology, University of Wisconsin School of Medicine and Public Health, Madison, WI 53705, USA. [2]Genetics Training Program, University of Wisconsin-Madison, Madison, WI 53703, USA. [3]Cell and Molecular Biology Training Program, University of Wisconsin-Madison, Madison, WI 53705, USA. [4]Department of Pathology, University of Michigan, Ann Arbor, MI 48109, USA.

*Author for correspondence (wellik@wisc.edu)

C.G.K.F., 0000-0001-5811-7269; P.R.V.G., 0000-0002-3175-8944; K.A.H., 0000-0002-8226-2033; D.M.W., 0000-0003-4078-8560

Handling Editor: Ken Poss
Received 14 June 2022; Accepted 13 January 2023

Development (2023) 150, dev201026. doi:10.1242/dev.201026

2017). How or whether these interstitial cell populations are distinct from one another is not fully understood, although there is at least some overlap between most of these subsets (Malecova and Puri, 2012; Tedesco et al., 2017). Previous work has shown that interstitial stromal cells support myofiber function and regeneration at adult stages, and can impact satellite cell quiescence, activation and migration (Heredia et al., 2013; Joe et al., 2010; Kuswanto et al., 2016; Murphy et al., 2011; Nassari et al., 2017; Tatsumi et al., 2009; Thomas et al., 2015; Tidball and Villalta, 2010; Uezumi et al., 2010).

A small but growing number of publications have reported that subsets of interstitial cells possess myogenic potential, but the *in vivo* myogenic potential of these cells remains controversial (Dellavalle et al., 2011; Doyle et al., 2011; Esteves de Lima et al., 2021; Giordani et al., 2019; Liu et al., 2017; Mierzejewski et al., 2020b; Mitchell et al., 2010; Qu-Petersen et al., 2002). Twist2-directed genetic lineage labeling from an interstitial cell subpopulation demonstrated a direct contribution to adult skeletal muscle fibers *in vivo* (Liu et al., 2017). Recently, it was reported that early lateral plate lineage cells from a *Scx-Cre* reporter show a contribution to muscle fibers and some of the satellite cell population, specifically at the myotendinous junction during embryogenesis (Esteves de Lima et al., 2021).

In this study, we employ our previously validated *Hoxa11eGFP* reporter and *Hoxa11-CreERT2* in combination with *ROSA26-LSL-tdTomato* and *ROSA26-LSL-H2BmCherry* lineage reporters to examine Hoxa11 expression and the lineage contribution from Hox-expressing muscle interstitial cells from embryonic to adult stages (Blum et al., 2014; Madisen et al., 2010; Nelson et al., 2008; Pineault et al., 2019). We demonstrate that Hoxa11eGFP expression is restricted to a subset of zeugopod-attached muscle interstitial cells from embryonic through adult stages. Flow cytometry and immunofluorescent analyses show that Hoxa11-expressing cells are a non-hematopoietic, non-endothelial, non-satellite cell stromal population with strong overlap with Twist2 and partial overlap with PDGFRα. Analysis from publicly available single-cell RNA-sequencing datasets of resident skeletal muscle mononuclear cells also demonstrate that *Hoxa11* is primarily expressed within fibroblasts where high Twist2 and PDGFRα expression is also observed. *Hoxa11-CreERT2* lineage induction from any stage results in initiation of labeling only in interstitial cells, as expected. Lineage induction at E12.5 results in restriction of lineage expression only in the muscle interstitial cells throughout the remainder of embryonic development. However, at postnatal and adult stages, the Hoxa11-expressing interstitial cell lineage begins showing lineage contribution to myofibers. This contribution is progressive; lineage reporter expression increases in skeletal muscle fibers in the weeks after induction. In parallel experiments comparing *Hoxa11-CreERT2* and *Pax7-CreERT2* to induce lineage labeling from the same *ROSA26-LSL-tdTomato* reporter, Hoxa11 lineage contribution is significantly higher than Pax7-expressing satellite cell contribution to forelimb muscles during adult homeostasis. Intriguingly, the extent of *Hoxa11*-mediated lineage labeling varies in a reproducible pattern in different muscle groups, even though *Hoxa11*-expressing interstitial cells are present in all zeugopod-attached muscles. Contribution of *Hoxa11*-expressing interstitial cell nuclei to muscle fibers was further validated by using a *Hoxa11-CreERT2; ROSA-LSL-H2BmCherry* reporter. Using this reporter, we demonstrate that Hoxa11-expressing interstitial cells contribute labeled nuclei to myofibers. The Hoxa11 lineage reporters do not mark Pax7-expressing satellite cells at any time point, supporting a *Hox11*-expressing cell contribution to myofibers that is independent of the satellite cell pool. We further assessed the myogenic potential of Hoxa11-lineage labeled cells *in vitro* and found that these cells are not capable of forming myotubes alone but can contribute to differentiating myotubes from canonical sources. Consistent with these findings, Hoxa11-lineage labeled cells do not contribute to newly injured myofibers, only beginning to contribute when regenerated myofibers are present. Taken together, these data support Hoxa11-expressing interstitial cells as a population of non-satellite cell muscle progenitors. This report adds to the growing evidence for non-satellite cell sources of muscle progenitors *in vivo* in mammals.

RESULTS

Hoxa11eGFP expression is maintained in skeletal muscle interstitial cells through postnatal and adult stages

During development, Hoxa11eGFP expression in muscle is restricted to the zeugopod-attached muscles, specifically in the non-endothelial interstitial stroma (Swinehart et al., 2013). We examined expression at embryonic, postnatal and adult stages in mice (*Mus musculus*), and observed that expression is maintained through postnatal and adult stages in zeugopod-attached skeletal muscle interstitial cells (Fig. 1A, Fig. S1A). A high proportion of interstitial cells are Hoxa11eGFP^{+} at embryonic and early postnatal stages. By adult stages, Hoxa11eGFP-expression is observed in a smaller proportion of interstitial cells, a point that warrants further future investigation. Using our previously validated *Hoxa11-CreERT2* to induce recombination of a *ROSA26-Lox-STOP-Lox-tdTomato* lineage reporter (referred to as Hoxa11iTom throughout; Madisen et al., 2010; Pineault et al., 2019), we observe that 3 days after a single 5 mg tamoxifen dose, Hoxa11iTom^{+} cells are distributed throughout the interstitial cells of all forelimb muscles (Fig. 1B, Fig. S1B). The Hoxa11iTom lineage is induced at ∼90% efficiency at this tamoxifen dose and overlaps with Hoxa11eGFP live reporter expression, validating our lineage reporter in this tissue (Fig. 1C, Fig. S2). Three days after the initiation of lineage labeling, Hoxa11iTom expression is observed only in the interstitial cells (Fig. 1B, Figs S1, S3).

Hoxa11eGFP-expressing cells are a non-hematopoietic, non-endothelial and non-satellite cell sub-population of muscle interstitial cells

Hoxa11iTom^{+} cells were assessed by flow cytometry, 4 days after a single 5 mg dose of tamoxifen, to investigate how they correlate with previously described populations of mononuclear stromal cells present in skeletal muscle. Live mononucleated cells were enzymatically isolated from limb muscles attached to the zeugopod and cells were gated for CD45 and CD31 to identify hematopoietic and endothelial cells. Hoxa11iTom cells were essentially absent from the blood lineage and endothelial population, as reported for Hoxa11-expressing skeletal stromal cells (Rux et al., 2016) (Fig. S4A). Of the non-hematopoietic non-endothelial population, fewer than 8% of remaining cells were Hoxa11iTom positive. Cells were further gated to identify FAPs and SMMCs using the Sca1, VCAM1 and ITGA7 cell surface markers (Giordani et al., 2019; Joe et al., 2010; Liu et al., 2013). Most non-hematopoietic non-endothelial cells are Sca1 negative in both the Hoxa11iTom^{+} (>79%) as well as the non-tdTom (75%) fraction, while 20% of Hoxa11iTom+ cells segregate as Sca1^{+} (Fig. 2A). Within this Sca1^{+}/Hoxa11iTom^{+} population, 52% of Hoxa11iTom^{+} cells are ITGA7 negative, correlating with previously identified FAPs (CD45^{+}/CD31^{-}/Sca1^{+}/ITGA7^{-}; Joe et al., 2010). A small fraction of the total Hoxa11iTom^{+} cell population (∼5%) segregated as CD45^{-}/CD31^{-}/Sca1^{-}/ITGA7^{+}/VCAM1^{-}, markers that have recently been reported to

Development (2023) 150, dev201026. doi:10.1242/dev.201026

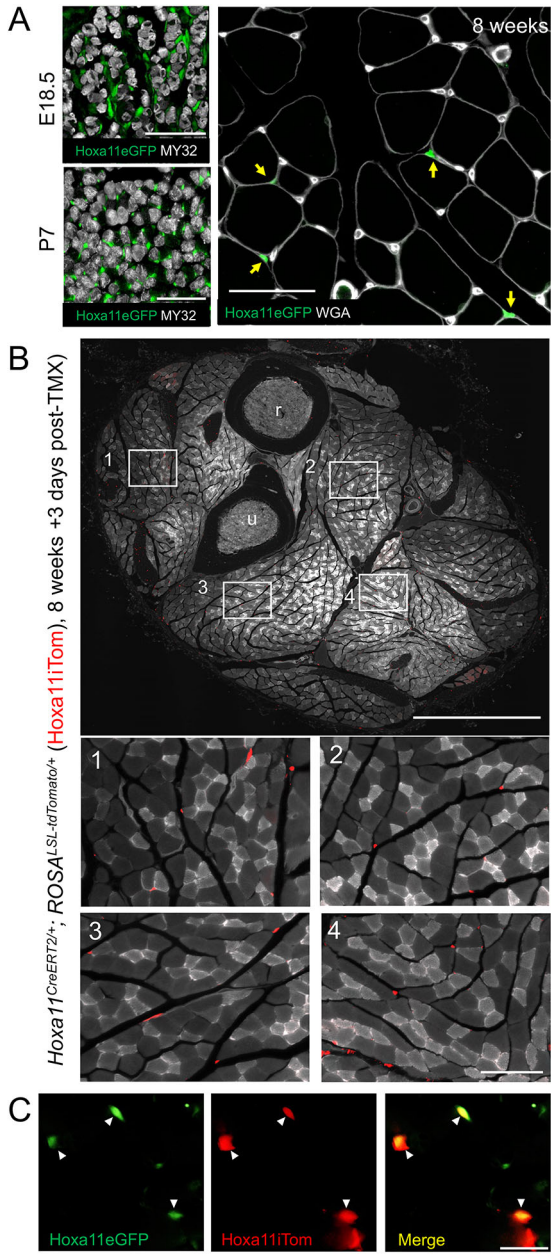

Fig. 1. Hoxa11 expression is maintained in skeletal muscle interstitial cells through adult stages. (A) Left: Hoxa11eGFP real-time reporter shows expression (green) at E18.5 and P7 in cells surrounding muscle fibers (MY32, white). Scale bars: 100 µm. *n*=3 for each time point. Right: at 8 weeks of age, Hoxa11eGFP (green, yellow arrows) is expressed in interstitial cells (WGA, white). Scale bar: 50 µm. *n*=6 animals. (B) A whole forelimb cross-section showing tdTomato expression (Hoxa11iTom, red) in interstitial cells throughout forelimb muscles. The areas outlined are shown underneath at higher magnification. Scale bars: 1000 µm and 100 µm, respectively. *n*=4 animals. (C) Hoxa11iTom (red) overlaps real-time reporter Hoxa11eGFP (green); white arrowheads indicate interstitial cells 48 h post-tamoxifen induction of Hoxa11iTom. Scale bar: 50 µm. *n*=2 animals. Positions of radius and ulna are marked by r and u, respectively.

be a sub-population of interstitial SMMCs that possess myogenic potential (Giordani et al., 2019). To further assess the Hox11-expressing cell population, we analyzed a publicly available dataset (Giordani et al., 2019). For these analyses, we merged two biological replicates from mouse hindlimb muscle (GSM3520458 and GSM3520459), normalized this merged dataset and removed low-quality and/or dying cells. The data were then projected by UMAP for visualization of distinct cell populations (clusters) (Fig. 2B). Cell-specific markers used by Giordani et al. were used to identify the clusters (Fig. 2C and Fig. S4) (Giordani et al., 2019). A feature plot showing the expression of *Hox11* genes among mononuclear muscle cells show a preponderance of this expression in fibroblasts and in tenocytes (Fig. 2D). A similar profile is observed for Twist2 and PDGFRα (Fig. 2E, Fig. S4). In contrast, Pax7 and Myod1 are predominantly found in satellite cells, although expression is observed in other subsets to varying degrees (Fig. 2E,F and Fig. S4) (Giordani et al., 2019).

We further characterized Hoxa11eGFP-expressing cells *in situ* by co-immunofluorescent immunohistochemistry. Hoxa11eGFP expression is observed in interstitial cells outside the basal lamina of myofibers and shows no overlap with satellite cells, based on Pax7 and laminin immunostaining (Fig. 2G). The transcription factor Twist2 is expressed in interstitial cells that possess previously reported myogenic potential (Li et al., 2019; Liu et al., 2017); we observe that most Hoxa11eGFP-expressing cells also express Twist2, although the two populations are not completely overlapping (Fig. 2H). Within the interstitial population, Hoxa11eGFP also shows partial overlap with PDGFRα, a marker used to identify FAPs (Joe et al., 2010; Mathew et al., 2011; Murphy et al., 2011; Uezumi et al., 2010, 2011) (Fig. 2I). These results corroborate and extend flow cytometry and scRNA-seq analyses, and demonstrate that Hoxa11eGFP is expressed in a sub-population of muscle interstitial cells.

Hoxa11 lineage in muscle tissue remains restricted to interstitial cells during embryonic stages but begins contributing to myofibers at postnatal stages

We next sought to examine the lineage of the Hoxa11-expressing population. To assess embryonic lineage, pregnant dams were dosed with tamoxifen at E12.5 and the resulting *Hoxa11*$^{CreERT2/+}$; *ROSA*$^{LSL\text{-}tdTomato/+}$ embryos were collected at E18.5. Hoxa11iTom expression is observed exclusively in the interstitial and connective tissue cells of developing muscles (Fig. 3A), similar to previously reported Hox11eGFP expression (Swinehart et al., 2013). A recent report identified an unexpected contribution to the myogenic lineage from embryonic lateral plate mesoderm using both quail-chick chimeras and a *Scleraxis-Cre* allele, and reported *Scx-Cre*-mediated contribution to the embryonic myogenic lineage at or near the myotendinous junction (Esteves de Lima et al., 2021). We observe no such localization of Hoxa11iTom to myofibers at the myotendinous junction region at embryonic stages (Fig. S5).

Postnatal lineage was examined by dosing *Hoxa11*$^{CreERT2/+}$; *ROSA*$^{LSL\text{-}tdTomato/+}$ animals with tamoxifen on postnatal day 3 (P3) and collecting tissue at P7, P14 and P28 (Fig. 3B). Whole forelimb cross-sections and higher magnification images show Hoxa11iTom expression within tendon, bone and muscle at all time points. Hoxa11iTom is expressed throughout the zeugopod forelimb in muscle interstitial cells at P7. At this time point, very low levels of tdTomato expression can be observed in a small number of myofibers (Fig. 3C). Images of P7, P14 and P28 taken at the same exposure show increasing number and intensity of tdTomato^{+} myofibers with time after induction (Fig. 3C).

Hoxa11-expressing cells make progressive contribution to adult skeletal myofibers at homeostasis and to a greater extent than *Pax7* lineage-induced satellite cells

To assess Hoxa11 lineage behavior at adult stages, *Hoxa11*$^{CreERT2/+}$; *ROSA*$^{LSL\text{-}tdTomato/+}$ animals were dosed with 5 mg tamoxifen at

Development (2023) 150, dev201026. doi:10.1242/dev.201026

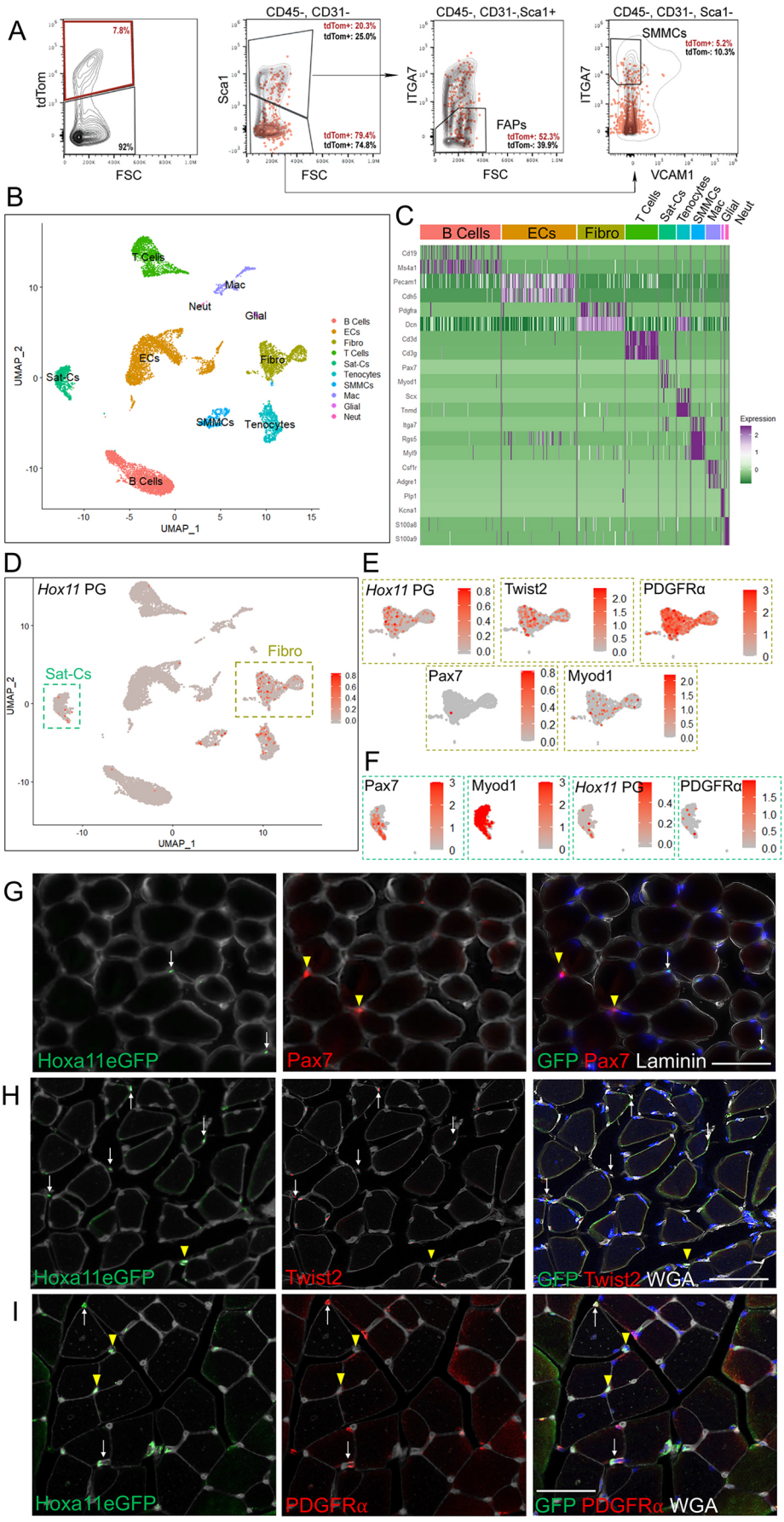

Fig. 2. Defining Hoxa11-expressing interstitial cells. (A) Hoxa11iTom$^+$ cells dotted (red) over a contour plot of non-tdTom cells. Flow cytometry of Hoxa11 lineage labeled cells (Hoxa11iTom) shows that Hoxa11iTom$^+$ cells are 7.8% of the mononuclear cells enzymatically isolated from zeugopod-attached muscles. Nearly 80% of the Hoxa11iTom$^+$ cells are Sca1$^-$. *n*=2 biological replicates. Among the 20% of Hoxa11iTom$^+$ cells that are Sca1$^+$, approximately half are ITGA7$^-$, which is a measure of fibroadipogenic progenitors (FAPs). Among the Sca1$^-$ population, ∼5% are ITGA7$^+$, which is a measure of smooth muscle mesenchymal cells (SMMCs). (B-F) These analyses merge two biological replicates from publicly available single cell sequencing data from adult mouse muscle mononuclear cells (GEO databases GSM3520458/GSM3520459). R studio (v 4.1.3) and Seurat (v 4.1.0) standard workflow were used for analyses. (B) After normalization and mitochondrial filtering (8%), the FindVAriableFeatures function was used before PCA (Dims=1:20) and the data were projected in a low-dimensional space via UMAP (resolution=0.5). (C) Two features per cluster were selected for visualization via a heatmap, as a secondary means of validating cluster identity and feature specificity. (D) Visualization of the expression of the Hox11 paralogous genes (PGs; *Hoxa11*, *Hoxc11* and *Hoxd11*) is shown. The fibroblast and satellite cell clusters were subsetted for higher magnification and resolution, and feature plots for additional interstitial cell markers (Twist2 and PDGFRα) and satellite/myoblast markers (Pax7 and Myod1) are shown (E,F). Immunofluorescent immunohistochemistry for GFP (Hoxa11eGFP, green) and for Pax7 (G, red), Twist2 (H, red) and PDGFRα (I, red) show no overlap between Hoxa11eGFP and Pax7, high overlap with Twist2, and a moderate level of overlap with PDGFRα. Scale bars: 50 µm. *n*=3 animals (G-I).

Development (2023) 150, dev201026. doi:10.1242/dev.201026

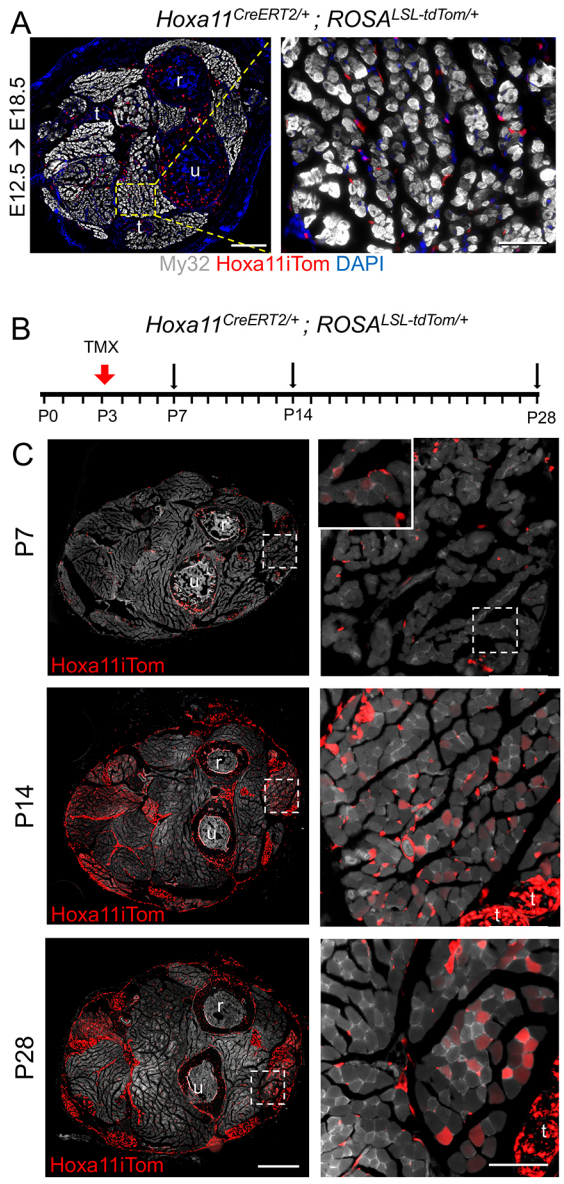

Fig. 3. Embryonic *Hoxa11* lineage-labeled cells remain exclusively interstitial; Hoxa11 lineage begins to show contribution to myofibers at postnatal stages. (A) After Hoxa11iTom induction at embryonic day (E) 12.5 and embryo collection at E18.5, representative cross-sections show Hoxa11iTom visible only in interstitial cells of the muscle (My32, white; DAPI, blue). Scale bars: 200 µm (left) and 50 µm (right). (B) At postnatal day (P) 3, Hoxa11$^{CreERT2/+}$; ROSA$^{LSL\text{-}tdTom/+}$ mice were given 0.25 mg tamoxifen by intragastric injection and collected at P7, P14 and P28. (C) Full forelimb cross-sections show Hoxa11iTom (red) expression at P7, P14 and P28 (left). Areas outlined in the images on the left are shown at higher magnification on the right. The inset in the top right image shows the area outlined at higher magnification. Scale bars: 500 µm (left) and 100 µm (right). *n*=3 for each time point. Radius, ulna and tendon position are marked by r, u and t, respectively.

8 weeks of age and analyzed at 2, 4, 7, 14 and 56 days after tamoxifen induction (Fig. 4A). At 4 days post-induction, there is extensive lineage labeling of muscle interstitial cells and only faint tdTomato signal in a few muscle fibers. At continuing time points through 8 weeks post-induction, lineage contribution to muscle fibers progressively increases, as seen in whole forelimb cross-sections and magnifications of three different muscles (Fig. 4B). Continual, progressive and more-extensive lineage labeling is observed at later stages (Fig. S6). The extent of lineage labeling in each muscle group varies, but with high reproducibility between animals. In Hoxa11iTom animals at 8 weeks after induction, the extensor carpi ulnaris (ECU) shows 95.2±2.9% tdTomato-positive fibers, the flexor digitorum profundus (FDP) shows 51.2±6.9% tdTomato-positive muscle fibers, and the flexor digitorum sublimis (FDS) has 20.5±4.9% tdTomato-positive fibers. Despite differential lineage labeling into muscle groups, Hoxa11iTom-labeled interstitial cells are observed relatively uniformly throughout forelimb muscle tissue (Fig. 1B; Figs S1, S3). Hindlimbs from these animals were also examined and Hoxa11iTom^{+} lineage contribution is observed (high levels of contribution to the gastrocnemius, moderate contributions to the tibialis anterior and low contribution to the soleus; Fig. S7).

Parallel experiments were performed using *Pax7*$^{CreERT2/+}$; *ROSA*$^{LSL\text{-}tdTomato/+}$ mice (Pax7iTom) (Murphy et al., 2011) to compare Hoxa11 lineage contribution to satellite cell contribution at homeostasis. Animals were given the same tamoxifen treatment, and this resulted in ∼90% efficient recombination in the *Pax7*$^{CreERT2/+}$; *ROSA*$^{LSL\text{-}tdTomato/+}$ animals (Fig. S2). The observed lineage contribution of Pax7-expressing satellite cells was significantly less than from Hoxa11-expressing cells (Fig. 4B-D). Of note, Pax7 lineage contribution was more evenly distributed throughout the muscle groups, with low but consistent increases in the amount of lineage-labeled myofibers over time, consistent with findings reported previously in the hindlimb (Fig. 4C) (Keefe et al., 2015; Pawlikowski et al., 2015). In examining the same three muscle groups, Pax7iTom contribution is 15.7±3.3% in the ECU, 21.5±3.1% in the FDP and 16.4±2.1% in the FDS. High-magnification images of the ECU, FDP and FDS muscle from Pax7iTom animals are shown in Fig. S8. Comparative quantification of lineage-positive myofibers of the FDP, ECU and FDS from both Hoxa11iTom and Pax7iTom animals at 8 weeks after induction shows Hoxa11iTom contribution is significantly higher in both the FDP and ECU muscles (Fig. 4D).

Our results show many similarities to those reported for Twist2-expressing interstitial cells (Liu et al., 2017) and, intriguingly, Hoxa11eGFP and Twist2 expression highly overlap. We sought next to interrogate whether this cellular lineage behavior occurs from other populations of muscle interstitial cells. PDGFRα is a more broadly expressed interstitial cell marker, so we used a *PDGFRα-CreERT2* and the *ROSA-LSL-tdTomato* reporter (PDGFRαiTom) to investigate the lineage contribution to myofibers (Rivers et al., 2008). Using this model, we do not observe lineage labeling into myofibers, even 10 weeks after adult induction (Fig. 4E). Of note, there is previously reported evidence that tdTomato mRNA can be packaged in extracellular vesicles that enter the myofiber, resulting in fusion-independent lineage reporter expression within muscle fibers (Murach et al., 2020). Close examination of the PDGFRαiTom shows a small number of myofibers (approximately five in a whole forelimb cross-section) with low levels of red fluorescence, perhaps indicative of this type of non-specific release and uptake of tdTomato RNA or protein (Fig. 4E). However, the relative lack of myofiber lineage labeling in the PDGFRαiTom animals supports that lineage contribution in the Hoxa11iTom model does not result from leaky expression or fusion of cytoplasmic vesicles.

Hoxa11 lineage demonstrates nuclear contribution to myofibers

We next generated a *Hoxa11*-dependent nuclear lineage reporter by crossing our *Hoxa11-CreERT2* line with *ROSA-LSL-H2BmCherry* (Blum et al., 2014). Resulting *Hoxa11*$^{CreERT2/+}$; *ROSA*$^{LSL\text{-}H2B\text{-}mCherry/+}$

Development (2023) 150, dev201026. doi:10.1242/dev.201026

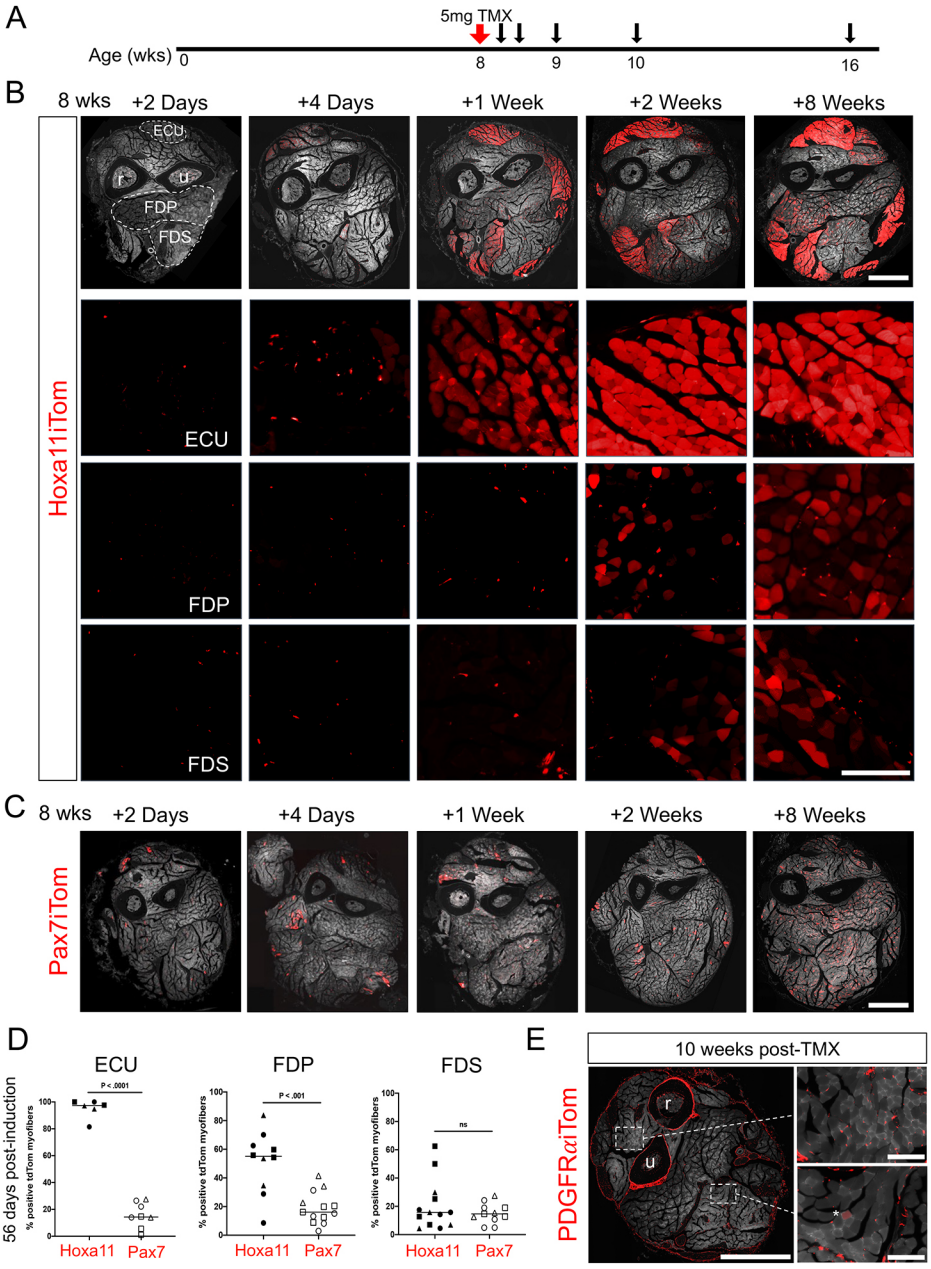

Fig. 4. Hoxa11-expressing skeletal muscle interstitial cells progressively contribute to myofibers in the adult mouse forelimb. (A) *Hoxa11*$^{CreERT2/+}$; *ROSA*$^{LSL\text{-}TdTom/+}$ (Hoxa11iTom) mice were given a single intraperitoneal injection of 5 mg tamoxifen at 8 weeks of age and collected at 2 days, 4 days, 1 week, 2 weeks and 8 weeks after tamoxifen induction. (B) Whole forelimb cross-sections were collected at the time points indicated. High-magnification images of the extensor carpi ulnaris (ECU), flexor digitorum profundus (FDP) and flexor digitorum sublimis (FDS) muscles show an increasing number of tdTomato-expressing myofibers over the indicated time points. Scale bars: 1000 µm (top); 200 µm (bottom). *n*=4 (2 days, 4 days and 8 weeks), 3 (7 days) and 9 (2 weeks) animals per time point. (C) Full forelimb cross-sections from *Pax7*$^{CreERT2/+}$; *ROSA*$^{LSL\text{-}TdTom/+}$ (Pax7iTom) animals show fewer tdTomato-positive myofibers compared with Hoxa11iTom animals at the same time points. Scale bar: 1000 µm. (D) Quantification of the percentage tdTomato-positive myofibers from ECU, FDS and FDP muscles from Hoxa11iTom and Pax7iTom animals 8 weeks post-induction. *n*=3 animals, two to five fields of view per muscle group analyzed. An unpaired Student's *t*-test was used to test for significance. ns, not significant. The white dashed line in B marks the borders of muscles that are quantified in D; the positions of the radius and ulna are marked by r and u, respectively. (E) *PDGFRα*$^{CreERT2/+}$; *ROSA*$^{LSL\text{-}tdTomato/+}$ (PDGFRαiTom) animals were also treated with 5 mg tamoxifen at 8 weeks of age and collected 10 weeks later. A whole cross-section of the forelimb shows tdTomato expression in connective tissues, bone tissue, tendons and the muscle interstitium. High-magnification images of skeletal muscle show PDGFRαiTom expression in the muscle interstitium. A few myofibers have low tdTomato expression (marked by an asterisk). Scale bars: 1000 µm (left); 100 µm (right). *n*=5 animals.

(Hoxa11iH2BmCherry) animals were given 5 mg tamoxifen at 6 weeks of age and collected at 4 days and 2 weeks after induction (Fig. 5A). H2BmCherry-labeled myonuclei are clearly observed in muscle interstitial cells 4 days after tamoxifen induction (Fig. 5B). By 2 weeks after lineage induction, Hoxa11iH2BmCherry^{+} nuclei can be additionally visualized within myofibers under the basal lamina (Fig. 5C). To confirm that Hoxa11iH2BmCherry^{+} nuclei under the basal lamina were indeed myonuclei, we performed dystrophin antibody staining and saw that many Hoxa11iH2BmCherry^{+} nuclei were inside the dystrophin layer and, therefore, in the myofibers (Fig. 5D). Hoxa11iH2BmCherry^{+} nuclei were confirmed with DAPI staining (Fig. S9). These experiments provide support for *Hoxa11*-expressing interstitial cells contributing full cellular contents, including their nuclei, to muscle fibers *in vivo*.

Hoxa11 lineage contributes to all muscle fiber types

Previous publications have reported that *Twist2*-mediated contribution to muscle exhibits fiber-type specificity, contributing to only Type IIb/x myofibers (Li et al., 2019; Liu et al., 2017). Of note, these experiments were conducted on animals that were lineage labeled for up to 4 months. Observation of the Hoxa11iTom lineage in the hindlimb 3 weeks after adult induction supports this myofiber specificity, as almost no lineage labeling is observed in the soleus, which comprises mainly type 1 myofibers, whereas fairly extensive labeling is observed in the adjacent gastrocnemius, which is mainly type IIb and IIx myofibers (Fig. S7) (Burkholder et al., 1994). However, upon evaluation of myofiber type specificity in Hoxa11iTom lineage 8 months after induction of the reporter (10 months of age), Hoxa11 lineage contribution to all four muscle types, types I, IIa, IIb and IIx, is observed (Fig. 6A-D).

Development (2023) 150, dev201026. doi:10.1242/dev.201026

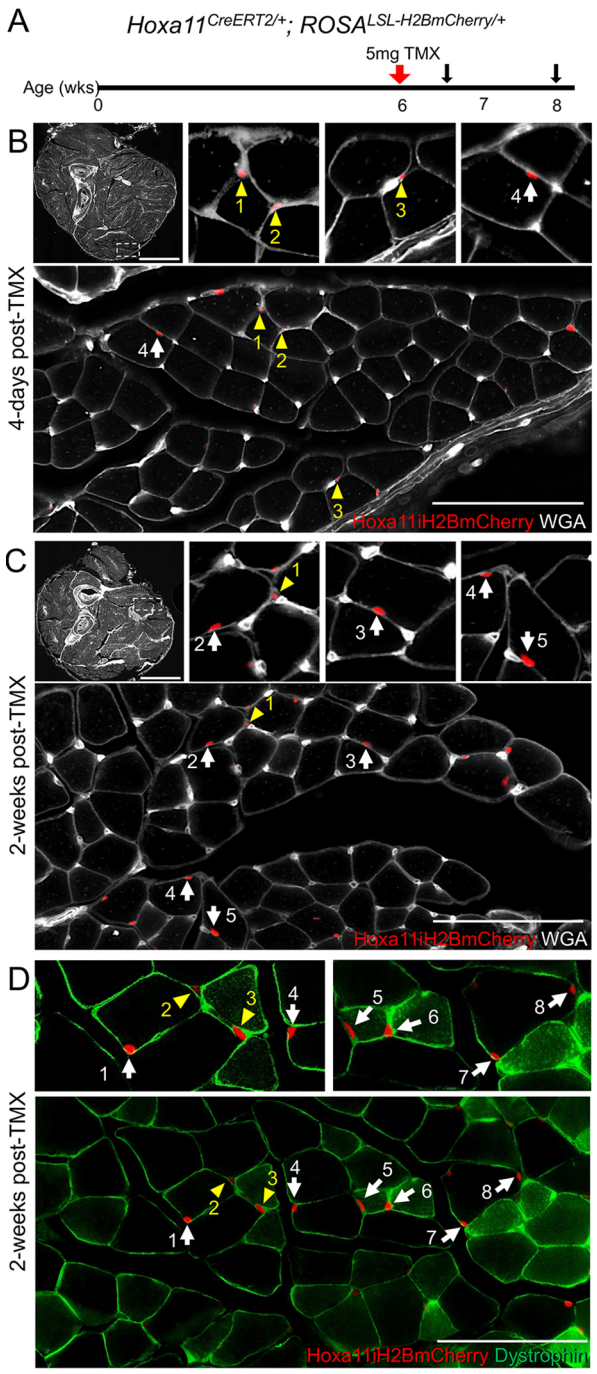

Fig. 5. Hoxa11-expressing interstitial cells contribute their nuclei to myofibers. (A) *Hoxa11*$^{CreERT2/+}$; *ROSA*$^{LSL\text{-}H2BmCherry/+}$ mice were given 5 mg of tamoxifen at 6 weeks of age and collected 4 days and 2 weeks later. (B,C) Whole forelimb cross-sections. Areas outlined in the top left are shown at higher magnification underneath. WGA (white) staining distinguishes mCherry (red) labeled myonuclei from labeled interstitial nuclei. Panels to the right of the whole forelimb cross-sections more clearly show the distinction between labeled interstitial nuclei and myonuclei. (B) Four days after tamoxifen treatment, the majority of labeled nuclei are interstitial; some labeled cells are myonuclei. (C) Two weeks after tamoxifen treatment, there are more labeled myonuclei and labeled interstitial nuclei are also visualized. Yellow arrowheads indicate mCherry-labeled interstitial cells; white arrows indicate mCherry-labeled myonuclei. Scale bars: 1000 µm (B,C). *n*=3 animals (4 day) and 2 animals (2 week). (D) Two weeks after tamoxifen treatment, mCherry-labeled myonuclei are observed within the dystrophin layer (white arrows), while interstitial cells are present outside the dystrophin layer (yellow arrowheads). Scale bar: 100 µm. *n*=2 animals.

Satellite cells are not lineage labeled by the *Hoxa11* lineage reporters

It is crucial to determine whether Hoxa11-mediated lineage labeling results in reporter expression in or through satellite cells. To rigorously assess for this, we examined co-expression of Pax7 and Hoxa11iTom in both the forelimb and the hindlimb of Hox11iTom animals. In the forelimb, the ECU, FDP and FDS were assessed for overlap of Hox11iTom and Pax7. We did not observe any instances of co-expression of Pax7 and Hoxa11iTom 2 weeks after induction out of a total of 1048 individual cells analyzed (Fig. 7A-D). We further assessed Hoxa11iTom and Pax7 antibody staining 8 weeks after lineage induction and again found no tdTomato^{+} satellite cells from 311 cells counted (Fig. S10). In the hindlimb, we analyzed three muscle groups, the gastrocnemius/plantaris, soleus and tibialis anterior for possible Hoxa11iTom and Pax7 co-expression.

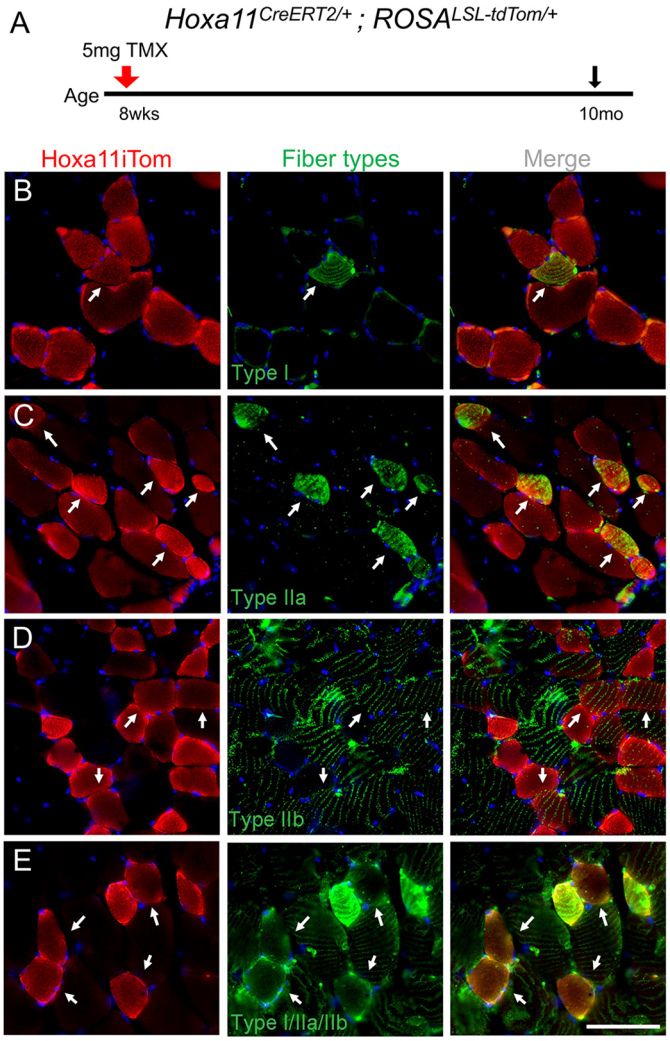

Fig. 6. Hoxa11iTom^{+} lineage shows contribution to all myofiber sub-types after 8 months of lineage labeling. (A) *Hoxa11*$^{CreERT2/+}$; *ROSA*$^{LSL\text{-}tdTom/+}$ mice were given 5 mg of tamoxifen at 8 weeks of age and collected at 10 months of age. (B-D) Hoxa11 lineage-labeled myofibers are identified by tdTomato signal (Hoxa11iTom). Myofiber sub-types were identified by immunofluorescent staining with anti-myosin (slow, Type I; B), anti-SC-71 (fast, Type IIa; C) and anti-BF-F3 (fast, Type IIb; D). (E) Type IIx fibers were identified by the absence of combined markers. Additional antibody details are available in Table S1. Fibers shown are from the gastrocnemius/plantaris muscles. White arrows indicate overlap of Hoxa11iTom and the specific myofiber type. Scale bar: 50 µm. *n*=3 animals.

Development (2023) 150, dev201026. doi:10.1242/dev.201026

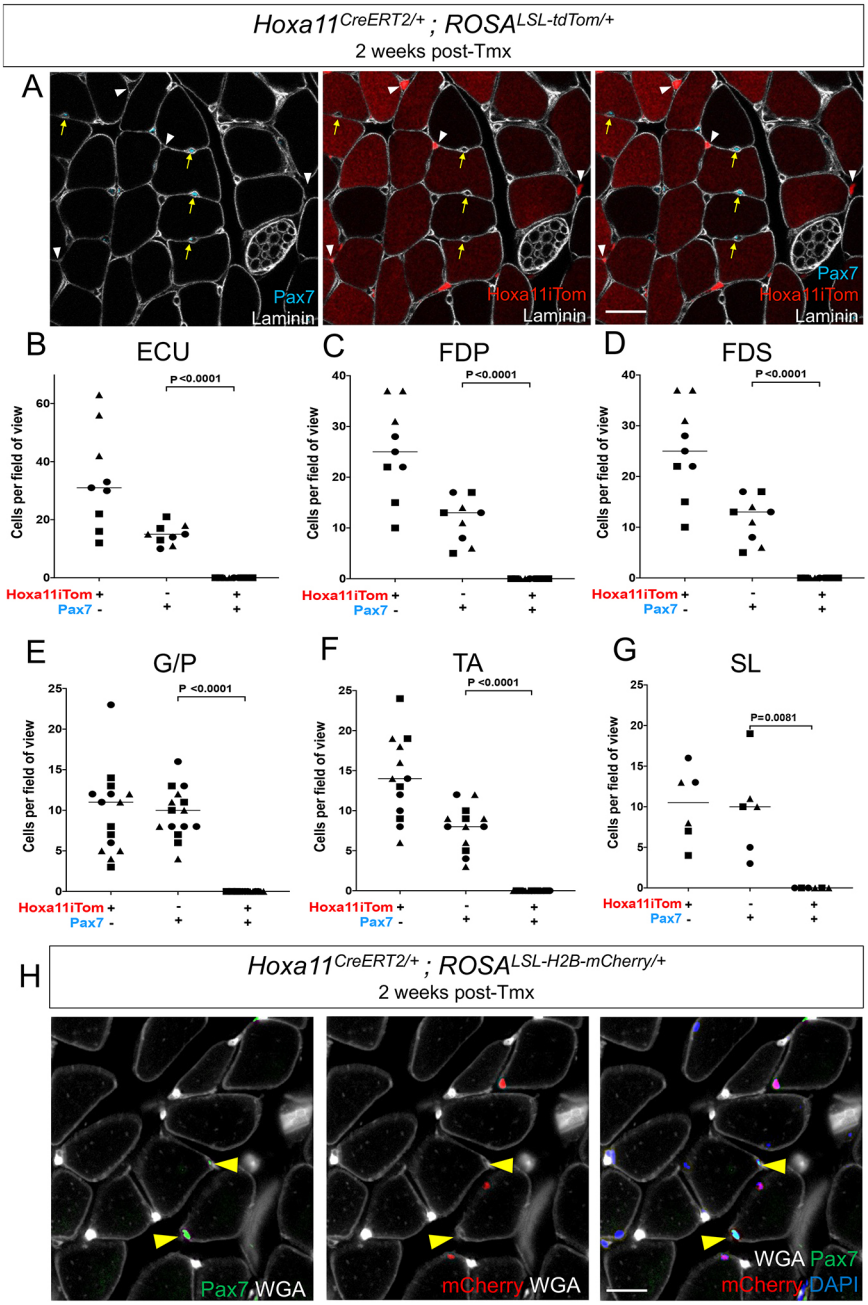

Fig. 7. *Pax7*-expressing satellite cells are not lineage labeled by the Hoxa11iTom lineage. (A) *Hoxa11*$^{CreERT2/+}$; *ROSA*$^{LSL\text{-}tdTom/+}$ mice given a single 5 mg dose of tamoxifen by intraperitoneal injection at 8 or 12 weeks of age were collected 2 weeks after dosing. Pax7^{+} satellite cells (cyan, yellow arrows) are visualized under the basal lamina (white) with zero incidences of Hoxa11 lineage labeling (red) of Pax7-expressing cells in forelimb skeletal muscle at 2 weeks post-induction. (B-D) Quantification of Hoxa11iTom^{+}, Pax7^{+} and overlapping cells in the extensor carpi ulnaris (ECU), flexor digitorum profundus (FDP) and flexor digitorum sublimis (FDS) is shown. *n*=3 animals. (E-G) Quantification of hindlimb muscles gastrocnemius/plantaris (G/P), and soleus (SL) and tibialis anterior (TA) muscles. There were no cells that expressed both Hoxa11iTom and Pax7. *n*=3 animals. Data are mean with individual data points indicated. Significance was tested using an unpaired Student's *t*-test. (H) *Hoxa11*$^{CreERT2/+}$; *ROSA*$^{LSL\text{-}H2B\text{-}mCherry/+}$ animals were mice given a single 5 mg dose of tamoxifen by intraperitoneal injection at 6 weeks of age and collected 2 weeks after tamoxifen administration. Pax7 antibody staining shows satellite cells are not mCherry^{+} in zeugopod attached muscles. *n*=2 animals. Yellow arrowheads indicate Pax7-stained satellite cells. Scale bars: 25 µm.

Consistent with data collected for the forelimb, no overlap of Hoxa11 lineage and Pax7 was observed in the 695 cells analyzed (Fig. 7E-G). Using our nuclear-specific reporter (Hoxa11-H2BmCherry), we assessed whether any Pax7^{+} cells were H2BmCherry^{+}. We observed no instances of Pax7^{+}/mCherry^{+} cells 2 weeks after reporter induction (Fig. 7H) These results indicate Hoxa11-expressing cells do not contribute to or non-specifically label the satellite cell population.

Hoxa11 lineage-labeled interstitial cells contribute to myotubes *in vitro*

To further test the myogenic potential of Hoxa11 interstitial cells, we examined their ability to form myotubes in culture. Hoxa11iTom^{+} cells were isolated from adult animals shortly after tamoxifen treatment (between 4 and 7 days after a 5 mg dose of tamoxifen) and sorted based on tdTomato^{+} fluorescence. Pax7iTom^{+} cells were isolated separately and run as positive controls. After 7 days in skeletal muscle differentiation medium (DM), Hoxa11iTom^{+} cells cultured alone failed to form any myotubes, in contrast to Pax7iTom^{+} cells, which show robust myotube formation (Fig. 8A,B). These results led us to examine whether Hoxa11iTom^{+} cells could contribute to existing myofibers. To test this, we differentiated C2C12 immortalized myoblasts in DM for 3-5 days (a point when myotube formation had initiated), then added either freshly isolated or previously cultured Hoxa11iTom^{+} cells. Extensive myotube formation was observed in wells containing only C2C12 cells (Fig. 8C). In wells containing both C2C12 with subsequent addition of Hoxa11iTom^{+} cells, we observed a subset of myotubes that became tdTom^{+} (Fig. 8D). Of note, not all myofibers became tdTomato^{+}, supporting cellular specificity of this contribution. Furthermore, many mononucleate Hoxa11iTom^{+} interstitial cells persisted in the culture, including

Development (2023) 150, dev201026. doi:10.1242/dev.201026

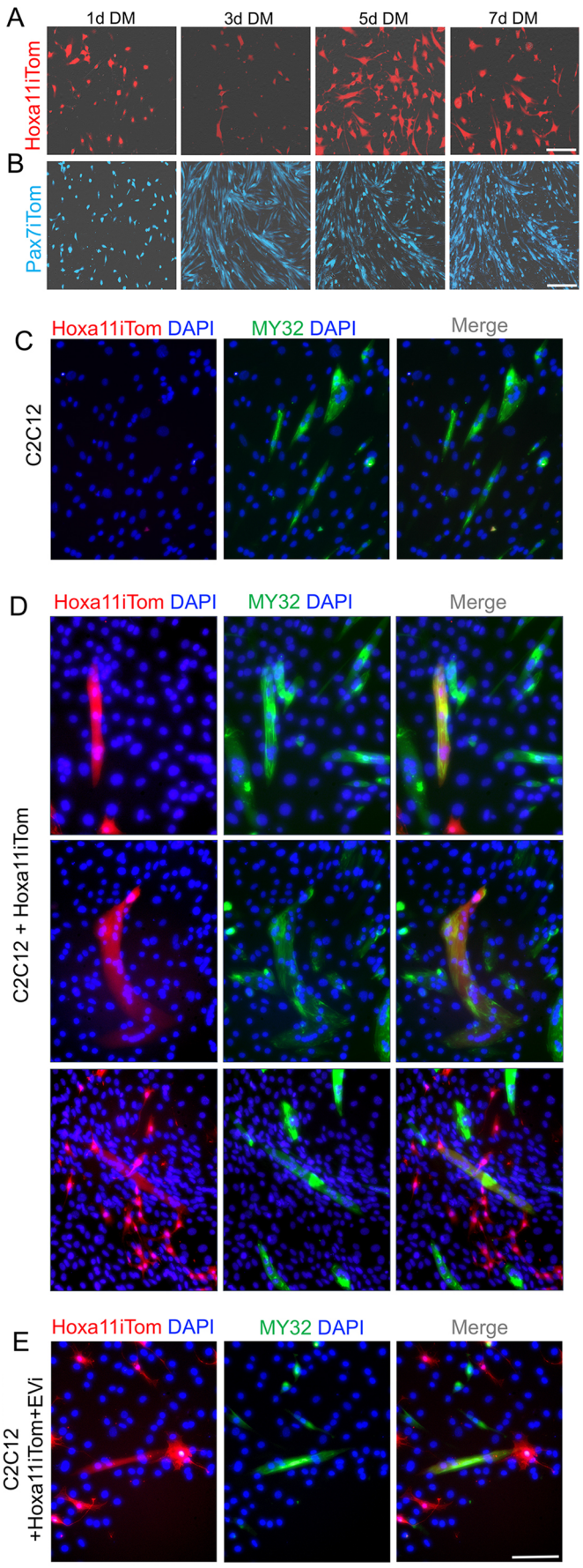

Fig. 8. Hoxa11iTom interstitial cells contribute to myotubes *in vitro*. Zeugopod-attached muscles from *Hoxa11*$^{CreERT2/+}$; *ROSA*$^{tdTomato/+}$ animals were enzymatically digested, and mononuclear cells were sorted to isolate Hoxa11iTom^{+} cells. (A) Hoxa11iTom^{+} cells (red) were cultured alone in muscle differentiation media (DM) and no myotube formation was observed after 7 days in culture. *n*=6 biological replicates. (B) In comparison, Pax7iTom cells (cyan) robustly form myotubes over 7 days in DM. *n*=3 biological replicates. (C-E) Fixed cells stained with MY32 (green) and DAPI (blue) shown with Hoxa11iTom (red) endogenous fluorescence overlapping multinucleated myosin-positive cells. (C) C2C12 immortalized myoblasts placed in DM for 9 days robustly form myotubes. (D) The contribution of Hoxa11iTom to myotubes is observed under conditions in which C2C12 cells are cultured in DM for 3 days then Hoxa11iTom^{+} interstitial cells are added for the remainder of the differentiation (+6 days). Notably, not all myotubes show contribution of tdTomato; additionally, many single tdTomato^{+} cells lie adjacent to differentiated myotubes with no red fluorescence. (E) The addition of an extracellular vesical inhibitor (EVi), Y-27632, at a concentration of 10 µM coincident with the addition of Hoxa11iTom^{+} cells on day 4 did not result in changes in tdTomato^{+} contribution to myotubes. Scale bars: 200 µm.

near myotubes that did not become tdTomato^{+}. These results strongly support direct contribution of the Hoxa11iTom^{+} cells to myofibers (not an indirect release of tdTomato mRNA or protein or other cytoplasmic contents into the medium and non-specific uptake into myofibers). To further examine the possibility of non-specific vesicle release of tdTomato, Y-27632 was added to C2C12/Hoxa11iTom^{+} combined cultures to prevent formation of extracellular vesicles (Kim et al., 2014; Tramontano et al., 2004; Watanabe et al., 2007). This treatment had no observable impact on tdTomato contribution to myofibers (Fig. 8E).

Hoxa11iTom contribution to regenerating myofibers after injury is delayed until myofiber regeneration has initiated

The contribution of Hoxa11-expressing cells to regenerating myofibers was examined by inducing the Hoxa11iTom lineage immediately before cardiotoxin injury of ventral, adult forelimb muscles (experimental strategy schematized in Fig. 9A). Comparison of the injured flexor carpi radialis (FCR) to the contralateral (uninjured) muscle from the same animals at 7 days post injury (DPI) shows very low Hoxa11 lineage contribution in the injured muscle whereas there are many tdTomato^{+} myofibers in the contralateral muscle (Fig. 9B). By 14 DPI, more tdTomato^{+} myofibers are observed in the injured muscle, notably in larger myofibers without apparent centralized nuclei, but also witnessed in a few myofibers with centralized nuclei (Fig. 9B). Many myofibers with centralized nuclei still lack tdTomato contribution at this stage. The contralateral muscle remains highly tdTomato positive at 14 DPI.

DISCUSSION

We have previously reported that Hoxa11eGFP is expressed broadly in embryonic interstitial cells of muscles attached to the zeugopod and function to pattern these muscles (Swinehart et al., 2013). In this report, we show that Hoxa11eGFP expression in muscle interstitial cells continues through postnatal and adult stages. And we show that lineage labeling using our previously validated Hoxa11CreERT2 allele faithfully initiates only in interstitial cells at all stages examined, as expected based on the expression of Hoxa11eGFP. Lineage-labeled cells remain interstitial throughout embryonic development, but beginning at postnatal stages, lineage labeling into myofibers is observed. At adult stages, lineage contribution to myofibers at homeostasis is quite robust and highly progressive, significantly exceeding the contribution of Pax7-mediated lineage labeling into myofibers.

Development (2023) 150, dev201026. doi:10.1242/dev.201026

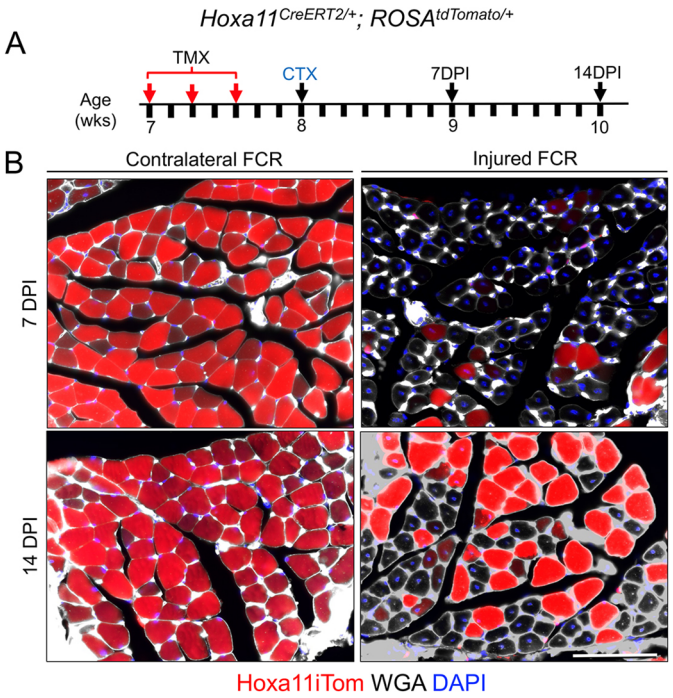

Fig. 9. Hox11 lineage makes minimal contribution to regenerating myofibers after injury. (A) *Hoxa11*$^{CreERT2/+}$*; ROSA*$^{tdTomato/+}$ adult animals were given three intraperitoneal (IP) injections of 2 mg tamoxifen (TMX) every other day in the week before cardiotoxin (CTX) injury. CTX injury was performed by injecting a total of 50 µl of 10 µM CTX into mouse forelimb muscles. Animals were collected 7 and 14 days post-injury (DPI). (B) The injured flexor carpi radialis (FCR) shows a very low contribution of tdTom to small injured myofibers with centralized nuclei compared with the contralateral (uninjured) FCR at 7 DPI. By 14 DPI, tdTom^{+} contribution to injured myofibers has increased, notably in larger myofibers without centralized nuclei. *n*=2 animals (four limbs for each time point). Scale bar: 100 µm.

This report follows other reports of possible non-satellite cell, i.e. muscle-resident cell populations with potential myogenic behavior. ‘Side population’ cells, pericyte or pericyte-like alkaline phosphatase-expressing cells, PW1^{+}/Pax7^{-} interstitial cells (PICs), CD146^{+} cells, Abcg2-labeled cells and ITGA7^{+}/VCAM^{-} SMMCs have all been reported to have myogenic activity (Dellavalle et al., 2011; Doyle et al., 2011; Giordani et al., 2019; Mierzejewski et al., 2020b; Mitchell et al., 2010; Qu-Petersen et al., 2002). These populations were intriguing, but their myogenic activity, in most cases, was not robust and was supported by little or no *in vivo* data.

A more rigorous report by Liu et al., using *Twist2*-directed genetic lineage labeling of interstitial cells, showed non-satellite cell contribution to myofibers at adult stages *in vivo*, highly consistent with our findings (Li et al., 2019; Liu et al., 2017). In this article, we show very similar lineage contribution from an independently generated, distinct genetic locus of another transcription factor (*Hoxa11*) that is expressed in a similar subset of muscle interstitial cells. As reported for *Twist2*, Hoxa11eGFP is expressed in only a subset of interstitial cells. *Twist2* and *Hoxa11*, at qualitative levels, are strongly overlapping; however, there are some incongruencies in our two reports. Liu et al. reported lineage-specific contribution to only type IIb and IIx fibers, whereas we show clear evidence of contribution to all four myofiber types. The differences may be due to timing: Twist2 lineage contribution to myofibers was assessed by fiber type 4 months after lineage induction, whereas we reported fiber sub-types 10 months after induction. Additionally, Hoxa11eGFP and Twist2 both overlap to some degree with other markers of interstitial cell subsets, such as PDGFRα, and this lineage does not show myofiber contribution. Further defining *Hoxa11*-expressing, *Twist2*-expressing and other interstitial cell populations will be crucial in future work to begin to dissect how myogenic potential is conferred.

The wealth of literature and decades of research on satellite cells and their crucial role as myofiber stem cells puts an exceedingly high burden of proof on new biology that suggests there may be an additional progenitor pool that is important during muscle homeostasis. As evidence has also been reported of non-specific cytoplasmic transport of fluorescent reporter mRNAs and proteins to other cells that refutes the results from our lineage reporters (Murach et al., 2020), we spent significant effort in testing this potential caveat to our results. First, we added an additional line of genetic experiments using the ROSA-LSL-H2BmCherry lineage reporter. Using this nuclearly localized lineage reporter, we show initial labeling in interstitial cell nuclei, but a relatively rapid and distinct contribution of H2BmCherry-labeled nuclei to muscle fibers. The specificity of *Hoxa11* (and *Twist2*) lineage contribution to myofibers is further supported by the lack of myofiber contribution observed with *PDGFRα-CreERT2*-induced lineage, even 10 weeks after induction. Particularly given the broader stromal expression of PDGFRα in muscle interstitial cells and connective tissue, if a non-specific mechanism were responsible for ‘tdTomato sharing’, one would expect it to occur with this Cre.

It is perhaps our *in vitro* work that most strongly supports the specificity of Hoxa11-expressing interstitial cell contribution to myofibers. Using FACS isolation of Hoxa11iTom cells and culturing them alone in muscle differentiation medium, we show very little to no ability of these cells to form myotubes. However, when we add Hoxa11iTom^{+} cells to differentiating myotubes from canonical sources (C2C12 cells), we see strong red fluorescence in some myotubes after several days of co-culturing. Crucially, not all myotubes show red fluorescence. In fact, many myotubes lying in close proximity to robustly red Hoxa11iTom^{+} mononuclear fibroblasts that persist in this co-culture show no detectable red fluorescence. This strongly argues against endovesicular release or non-specific uptake of cytoplasmic contents; if myotubes gained red fluorescence via these mechanisms, it would be more uniformly observed. Furthermore, the addition of an inhibitor of endovesicular release in this co-culture did not impact myofiber contribution.

An additional piece of evidence that supports the specificity and the nature of Hoxa11-expressing interstitial cell contribution to myofibers is our observation that little to no contribution of Hoxa11iTom is observed at early stages (7 days) after cardiotoxin injury. This type of injury leads to an acute disruption of cell membranes in the injured area. If myofibers were non-specifically labeled by released cytoplasmic contents, one certainly might imagine this would happen when myofiber membranes are damaged.

Our collective data, together with our observation that Hoxa11iTom^{+} contribution is observed again at 14 days post-injury in larger more-regenerated fibers is consistent with Hoxa11iTom^{+} interstitial cells being a post-embryonic myoprogenitor pool that lacks innate stem cell activity but serves as an important progenitor source of new myonuclei at homeostasis. This finding suggests a need for additional myonuclei during homeostasis. There are conflicting reports regarding the stability of myonuclear number in the absence of injury (Egner et al., 2016; Fry et al., 2015; Jackson et al., 2012; McCarthy et al., 2011; McLoon

Development (2023) 150, dev201026. doi:10.1242/dev.201026

and Wirtschafter, 2003; Murach et al., 2020; Pawlikowski et al., 2015; White et al., 2010). Our data, combined with the data from Twist2 lineage labeling, supports a model whereby turnover may be greater within type IIb and IIx myofibers, leading to higher homeostatic contribution in those fiber types. The issue of myonuclear turnover and potential changes in myonuclear number with age or under various conditions deserves rigorous attention. Of note, it will be critical for future investigations to account of the potential addition of myonuclei from non-satellite cell sources.

There are many lingering questions regarding the behavior and identity of Hoxa11-expressing cells in muscle. It will be interesting to examine the impact of depletion of Hoxa11-expressing cells on skeletal muscle homeostasis, growth and repair, and the degree of stem/progenitor ability they possess during aging, exercise, and in transplantation experiments. Perhaps the most exciting potential related to this understudied interstitial cell population and its ability to contribute to muscle fibers at homeostasis *in vivo* is the possibility that it could lead to new therapies for those suffering from myopathies and muscular dystrophies.

MATERIALS AND METHODS

Mouse models

Generation of mouse models *Hoxa11eGFP* (Nelson et al., 2008), *Hoxa11-CreERT2* (Pineault et al., 2019), *Pax7-CreERT2* (Murphy et al., 2011), *PDGFRα-CreERT2* (Rivers et al., 2008) and *ROSA-LSL-H2B-mCherry* (Blum et al., 2014) have been previously described. The *ROSA26-CAG-loxP-STOP-loxP-tdTomato* (stock number 007909; Madisen et al., 2010) was purchased from The Jackson Laboratory. Creation of *Hoxa11iTom* mice was achieved by crossing $Hoxa11^{CreERT2/+}$ males with $Hoxa11^{eGFP/+}$; $ROSA^{LSL\text{-}tdTomato/LSL\text{-}tdTomato}$ females. Generation of *Pax7iTom* mice was achieved by crossing $Pax7^{CreERT2/+}$ males with $ROSA^{LSL\text{-}tdTomato/LSL\text{-}tdTomato}$ females. All mouse colonies were maintained on a mixed genetic background. Both male and female mice were used in all experiments (and all control and mutant pairs were sex matched). Animals used in this study were euthanized using CO_2 followed by cervical dislocation. All procedures described were in compliance with protocols approved by the University of Wisconsin-Madison and the University of Michigan Animal Care and Use Committees.

Tamoxifen treatment

Adult mice were given a single intraperitoneal (IP) injection of 5 mg tamoxifen (Sigma-Aldrich T5648) dissolved in corn oil at 8 weeks of age and collected at indicated time points. Embryonic induction was achieved by mating $Hoxa11^{CreERT2/+}$ males to $Hoxa11^{eGFP/+}$; $ROSA^{LSL\text{-}tdTomato/LSL\text{-}tdTomato}$ females and the presence of vaginal plugs was checked each morning. Pregnant dams were given 2 mg tamoxifen and 0.1 mg progesterone dissolved in corn oil via IP injection at indicated embryonic time points (Pineault et al., 2019). Postnatal animals were given 0.25 mg of tamoxifen dissolved in corn oil via intragastric injection on postnatal day 3. Animals in the injury study were given three doses consisting of 2 mg tamoxifen via IP injection the week before injury.

Tissue preparation

Left and right zeugopods were collected. Skin and soft tissues were removed from the region and the zeugopod muscles and skeleton were isolated. Muscles were either carefully dissected off the bone or left attached to the bone. Dissection was carried out in phosphate-buffered saline (PBS). Muscle groups and intact limbs were fixed in 4% paraformaldehyde (PFA, Sigma-Aldrich) in PBS shaking at 4°C for 1-3 days. Intact limbs were decalcified in 14% ethylenediaminetetraacetic acid (EDTA, EMD Millipore) for 3-5 days (postnatal animals) or 6-7 days (adults) at 4°C. Samples were cryoprotected in 30% sucrose in PBS overnight before embedding in OCT compound (Thermo Fisher Scientific, 4585). Tissue was stored a −80°C. Cryosections of 10-14 µm were analyzed by IF.

Immunohistochemistry

Sections were rehydrated with PBS. In some cases, antigen retrieval was performed by heating slides in a citrate buffer for 10-30 min. After blocking with TNB buffer (Perkin Elmer, FP1020), sections were incubated with primary antibodies overnight at 4°C and then incubated with secondary antibodies for 2 h at room temperature and counterstained with DAPI for nuclear visualization. Antibody information is provided in Table S1. tdTomato and mCherry were visualized directly with no antibody staining. Slides were mounted with ProLong Gold antifade reagent (Invitrogen, cat. no. P36930). Staining using mouse monoclonal antibodies used a mouse-on-mouse immunodetection kit (Vector Labs, cat. no. BMK-2202) according to vendor instructions.

Imaging was performed on the Nikon eclipse Ti, Keyence BZ-X800 and Leica SP8 3X STED confocal. Image editing was performed using ImageJ and Photoshop, and larger images were stitched together (when necessary) in Photoshop or by the Keyence BZ-X800 analyzer.

Quantification

For calculation of percent $tdTomato^+$ myofibers from Hoxa11iTom and Pax7iTom mice, multiple representative fields of view, from the ECU, FDP and FDS muscles collected 8 weeks after Cre induction, were compiled. A blinded participant counted the total number of myofibers in the field of view and the total number of $tdTomato^+$ myofibers. Percent of $tdTomato^+$ myofibers was calculated; data were transferred to GraphPad Prism9 where statistical analysis for significance, between Hoxa11iTom and Pax7iTom ECU, FDP and FDS muscles, and the standard error was carried out. To assess the overlap of Hoxa11 lineage labeled cells with Pax7, tissue from Hoxa11iTom mice was collected at 2 weeks and 8 weeks post-induction; sections were stained using an anti-Pax7 antibody (DSHB). Three to five fields of view from each animal (n=3 for both forelimb and hindlimb analyses) were used; Pax7 and Hoxa11iTom cells were identified, counted and profiled into three groups: Hoxa11iTom+/Pax7-, Hoxa11iTom-/Pax7+ or Hoxa11iTom+/Pax7+. Statistical analyses were carried out using an unpaired Student's t-test (GraphPad Prism9).

Flow cytometry

To isolate mononuclear populations from muscle, we essentially followed the protocol of Liu et al. (2017). Briefly, zeugopod-attaching muscles were removed from the forelimb and hindlimb. Dissected muscles were chopped into smaller pieces followed by digestion in 700 U/ml collagenase type II (Gibco, 17101-015) at 37°C for 1 h. After wash and trituration steps, muscles underwent a second digestion in 100 U/ml collagenase type II and 1.1 U/ml dispase (Gibco, 17105-041) for 30 min at 37°C. Cells were washed and triturated, and red blood cell lysis was performed with an acidic salt solution. Cells were then filtered through a 40 µm cell strainer before being placed in 1×PBS with 2% FBS (Gibco). Flow cytometry experiments were carried out on the ThermoFisher Attune NxT Flow Cytometer BRYV. Antibody information is provided in Table S1. Analysis was carried out using FloJo.

Single cell RNA-sequencing analysis

Publicly available single cell sequencing data from adult mouse hindlimb were obtained from the GEO database (GSM3520458/GSM3520459) (Giordani et al., 2019). The two biological replicates were merged in R studio (v 4.1.3), and Seurat (v 4.1.0) (Hao et al., 2021) standard workflow was used for analysis. In brief, the data were normalized (min.cells=3, min.features=200, percent mitochondrial filtration <8%) to remove low-quality and dying cells. The FindVariableFeatures function was used before PCA, for which dims=1:20. This information was then used in a clustering algorithm (FindNeighbors, FindClusters) to project the data in a low-dimensional space via UMAP (resolution=0.5). Cluster identity was determined based on the list of cell-specific markers used previously (Giordani et al., 2019).

Cell culture

Cells were prepared as described above, and then sorted by FACS on a BD FACS Aria for tdTomato fluorescence. Both Hoxa11iTom and Pax7iTom

cells were grown in DMEM/F-12 supplemented with 10% FBS and 1% penicillin/streptomycin (Gibco, 11330057) to 70-80% confluence followed by the addition of skeletal muscle differentiation media [DM; DMEM (Gibco, 11885084) supplemented with 2% horse serum (Gibco, 26050070) and 1% penicillin/streptomycin (Gibco, 15140122)]. Medium was changed every other day. C2C12 cells (ATCC, validated and tested for contamination by source) were grown in DMEM supplemented with 10% FBS and 1% penicillin/streptomycin. Cells were grown to 70-80% confluence before being switched over to DM. After 3 days in DM, either freshly isolated or cultured (P1-P3) Hoxa11iTom cells were added to wells containing differentiating C2C12 cells. Medium was changed every other day. To inhibit formation of extracellular vesicles or micro vesicles, 10 µM of ROCK inhibitor, Y-27632, was added to DM in cultures containing C2C12 differentiating cells upon addition of Hoxa11iTom cells and maintained through the duration of the experiment. Differentiating cells were imaged (phase and tdTomato fluorescence channel) every 6-12 h using the Incucyte S3.

Cardiotoxin injury

Before injury, animals were given 5 mg/kg carprofen (Zoetis, Rimadyl) for pain management. Animals were anesthetized with 2-4% isoflurane. For injury, 50 µl of 10 µM cardiotoxin (Sigma-Aldrich, 217503-1MG; dissolved in normal saline) was injected directly into the ventral forelimb muscles of anesthetized animals. Muscles were collected 7 and 14 days after injury.

Acknowledgements

We sincerely thank and are grateful for assistance provided by Alex Hurley. We also thank Gabrielle Kardon (PhD) for providing the Pax7-CreERT2 mouse model and Barak Blum (PhD) for providing the ROSA-H2B-mCherry mouse model, without which this work would not have been possible. We are also very grateful to Troy Hornberger (PhD) for providing C2C12 immortalized myoblasts for our *in vitro* studies. The authors thank the University of Wisconsin-Madison Carbone Cancer Center Flow Cytometry Laboratory, supported by P30 CA014520, for use of its facilities and services.

Competing interests

The authors declare no competing or financial interests.

Author contributions

Conceptualization: D.M.W.; Methodology: C.G.K.F., P.R.V.G., Q.G.; Validation: C.G.K.F., P.R.V.G., Q.G.; Formal analysis: C.G.K.F., K.A.H.; Data curation: K.A.H.; Investigation: C.G.K.F., P.R.V.G., Q.G., S.M.H., A.E.M., A.M., A.P.M.; Writing - original draft: C.G.K.F.; Writing - review & editing: P.R.V.G., K.A.H., Q.G., D.M.W.; Visualization: C.G.K.F., P.R.V.G., S.M.H., A.P.M.; Supervision: D.M.W.; Project administration: D.M.W.; Funding acquisition: D.M.W.

Funding

This work was supported by the National Institutes of Health (R21 AR072511). Deposited in PMC for release after 12 months.

Data availability

All relevant data can be found within the article and its supplementary information. We used previously published sequencing data that has been deposited in GEO under accession numbers GSM3520458 and GSM3520459.

Peer review history

The peer review history is available online at https://journals.biologists.com/dev/article-lookup/doi/10.1242/dev.201026.reviewer-comments.pdf

References

Aoyama, H. and Asamoto, K. (1988). Determination of somite cells: independence of cell differentiation and morphogenesis. *Development* **104**, 15-28. doi:10.1242/dev.104.1.15

Blum, B., Roose, A. N., Barrandon, O., Maehr, R., Arvanites, A. C., Davidow, L. S., Davis, J. C., Peterson, Q. P., Rubin, L. L. and Melton, D. A. (2014). Reversal of β cell de-differentiation by a small molecule inhibitor of the TGFβ pathway. *eLife* **3**, e02809. doi:10.7554/eLife.02809

Burkholder, T. J., Fingado, B., Baron, S. and Lieber, R. L. (1994). Relationship between muscle fiber types and sizes and muscle architectural properties in the mouse hindlimb. *J. Morphol.* **221**, 177-190. doi:10.1002/jmor.1052210207

Chal, J. and Pourquié, O. (2017). Making muscle: skeletal myogenesis in vivo and in vitro. *Development* **144**, 2104-2122. doi:10.1242/dev.151035

Davis, A. P. and Capecchi, M. R. (1996). A mutational analysis of the 5′ HoxD genes: dissection of genetic interactions during limb development in the mouse. *Development* **122**, 1175-1185. doi:10.1242/dev.122.4.1175

Dellavalle, A., Maroli, G., Covarello, D., Azzoni, E., Innocenzi, A., Perani, L., Antonini, S., Sambasivan, R., Brunelli, S., Tajbakhsh, S. et al. (2011). Pericytes resident in postnatal skeletal muscle differentiate into muscle fibres and generate satellite cells. *Nat. Commun.* **2**, 499. doi:10.1038/ncomms1508

Doyle, M. J., Zhou, S., Tanaka, K. K., Pisconti, A., Farina, N. H., Sorrentino, B. P. and Olwin, B. B. (2011). Abcg2 labels multiple cell types in skeletal muscle and participates in muscle regeneration. *J. Cell Biol.* **195**, 147-163. doi:10.1083/jcb.201103159

Duprez, D. (2002). Signals regulating muscle formation in the limb during embryonic development. *Int. J. Dev. Biol.* **46**, 915-925.

Egner, I. M., Bruusgaard, J. C. and Gundersen, K. (2016). Satellite cell depletion prevents fiber hypertrophy in skeletal muscle. *Development* **143**, 2898-2906. doi:10.1242/dev.134411

Esteves de Lima, J., Blavet, C., Bonnin, M.-A., Hirsinger, E., Comai, G., Yvernogeau, L., Delfini, M.-C., Bellenger, L., Mella, S., Nassari, S. et al. (2021). Unexpected contribution of fibroblasts to muscle lineage as a mechanism for limb muscle patterning. *Nat. Commun.* **12**, 3851. doi:10.1038/s41467-021-24157-x

Fromental-Ramain, C., Warot, X., Lakkaraju, S., Favier, B., Haack, H., Birling, C., Dierich, A., Dollé, P. and Chambon, P. (1996a). Specific and redundant functions of the paralogous Hoxa-9 and Hoxd-9 genes in forelimb and axial skeleton patterning. *Development* **122**, 461-472. doi:10.1242/dev.122.2.461

Fromental-Ramain, C., Warot, X., Messadecq, N., LeMeur, M., Dollé, P. and Chambon, P. (1996b). Hoxa-13 and Hoxd-13 play a crucial role in the patterning of the limb autopod. *Development* **122**, 2997-3011. doi:10.1242/dev.122.10.2997

Fry, C. S., Lee, J. D., Mula, J., Kirby, T. J., Jackson, J. R., Liu, F., Yang, L., Mendias, C. L., Dupont-Versteegden, E. E., McCarthy, J. J. et al. (2015). Inducible depletion of satellite cells in adult, sedentary mice impairs muscle regenerative capacity without affecting sarcopenia. *Nat. Med.* **21**, 76-80. doi:10.1038/nm.3710

Giordani, L., He, G. J., Negroni, E., Sakai, H., Law, J. Y. C., Siu, M. M., Wan, R., Corneau, A., Tajbakhsh, S., Cheung, T. H. et al. (2019). High-dimensional single-cell cartography reveals novel skeletal muscle-resident cell populations. *Mol. Cell* **74**, 609-621.e606. doi:10.1016/j.molcel.2019.02.026

Goh, Q. and Millay, D. P. (2017). Requirement of myomaker-mediated stem cell fusion for skeletal muscle hypertrophy. *eLife* **6**, e20007. doi:10.7554/eLife.20007

Hao, Y., Hao, S., Andersen-Nissen, E., Mauck, W. M., III, Zheng, S., Butler, A., Lee, M. J., Wilk, A. J., Darby, C., Zager, M. et al. (2021). Integrated analysis of multimodal single-cell data. *Cell* **184**, 3573-3587.e3529. doi:10.1016/j.cell.2021.04.048

Heredia, J. E., Mukundan, L., Chen, F. M., Mueller, A. A., Deo, R. C., Locksley, R. M., Rando, T. A. and Chawla, A. (2013). Type 2 innate signals stimulate fibro/adipogenic progenitors to facilitate muscle regeneration. *Cell* **153**, 376-388. doi:10.1016/j.cell.2013.02.053

Jackson, J. R., Mula, J., Kirby, T. J., Fry, C. S., Lee, J. D., Ubele, M. F., Campbell, K. S., McCarthy, J. J., Peterson, C. A. and Dupont-Versteegden, E. E. (2012). Satellite cell depletion does not inhibit adult skeletal muscle regrowth following unloading-induced atrophy. *Am. J. Physiol. Cell Physiol.* **303**, C854-C861. doi:10.1152/ajpcell.00207.2012

Joe, A. W. B., Yi, L., Natarajan, A., Le Grand, F., So, L., Wang, J., Rudnicki, M. A. and Rossi, F. M. V. (2010). Muscle injury activates resident fibro/adipogenic progenitors that facilitate myogenesis. *Nat. Cell Biol.* **12**, 153-163. doi:10.1038/ncb2015

Keefe, A. C., Lawson, J. A., Flygare, S. D., Fox, Z. D., Colasanto, M. P., Mathew, S. J., Yandell, M. and Kardon, G. (2015). Muscle stem cells contribute to myofibres in sedentary adult mice. *Nat. Commun.* **6**, 7087. doi:10.1038/ncomms8087

Kim, M., Ham, A., Kim, K. Y.-M., Brown, K. M. and Lee, H. T. (2014). The volatile anesthetic isoflurane increases endothelial adenosine generation via microparticle ecto-5'-nucleotidase (CD73) release. *PLoS ONE* **9**, e99950. doi:10.1371/journal.pone.0099950

Kuswanto, W., Burzyn, D., Panduro, M., Wang, K. K., Jang, Y. C., Wagers, A. J., Benoist, C. and Mathis, D. (2016). Poor repair of skeletal muscle in aging mice reflects a defect in local, Interleukin-33-dependent accumulation of regulatory T cells. *Immunity* **44**, 355-367. doi:10.1016/j.immuni.2016.01.009

Lance-Jones, C. (1988). The effect of somite manipulation on the development of motoneuron projection patterns in the embryonic chick hindlimb. *Dev. Biol.* **126**, 408-419. doi:10.1016/0012-1606(88)90150-9

Lepper, C. and Fan, C.-M. (2010). Inducible lineage tracing of Pax7-descendant cells reveals embryonic origin of adult satellite cells. *Genesis* **48**, 424-436. doi:10.1002/dvg.20630

Lepper, C., Partridge, T. A. and Fan, C.-M. (2011). An absolute requirement for Pax7-positive satellite cells in acute injury-induced skeletal muscle regeneration. *Development* **138**, 3639-3646. doi:10.1242/dev.067595

Li, S., Karri, D., Sanchez-Ortiz, E., Jaichander, P., Bassel-Duby, R., Liu, N. and Olson, E. N. (2019). Sema3a-Nrp1 signaling mediates fast-twitch myofiber

specificity of Tw2(+) cells. *Dev. Cell* **51**, 89-98.e84. doi:10.1016/j.devcel.2019.08.002

Liu, L., Cheung, T. H., Charville, G. W., Hurgo, B. M. C., Leavitt, T., Shih, J., Brunet, A. and Rando, T. A. (2013). Chromatin modifications as determinants of muscle stem cell quiescence and chronological aging. *Cell Rep* **4**, 189-204. doi:10.1016/j.celrep.2013.05.043

Liu, N., Garry, G. A., Li, S., Bezprozvannaya, S., Sanchez-Ortiz, E., Chen, B., Shelton, J. M., Jaichander, P., Bassel-Duby, R. and Olson, E. N. (2017). A Twist2-dependent progenitor cell contributes to adult skeletal muscle. *Nat. Cell Biol.* **19**, 202-213. doi:10.1038/ncb3477

Madisen, L., Zwingman, T. A., Sunkin, S. M., Oh, S. W., Zariwala, H. A., Gu, H., Ng, L. L., Palmiter, R. D., Hawrylycz, M. J., Jones, A. R. et al. (2010). A robust and high-throughput Cre reporting and characterization system for the whole mouse brain. *Nat. Neurosci.* **13**, 133-140. doi:10.1038/nn.2467

Malecova, B. and Puri, P. L. (2012). "Mix of Mics"- phenotypic and biological heterogeneity of "Multipotent" Muscle Interstitial Cells (MICs). *J. Stem Cell Res. Ther.* **Suppl. 11**, 004. doi:10.4172/2157-7633.S11-004

Mathew, S. J., Hansen, J. M., Merrell, A. J., Murphy, M. M., Lawson, J. A., Hutcheson, D. A., Hansen, M. S., Angus-Hill, M. and Kardon, G. (2011). Connective tissue fibroblasts and Tcf4 regulate myogenesis. *Development* **138**, 371-384. doi:10.1242/dev.057463

McCarthy, J. J., Mula, J., Miyazaki, M., Erfani, R., Garrison, K., Farooqui, A. B., Srikuea, R., Lawson, B. A., Grimes, B., Keller, C. et al. (2011). Effective fiber hypertrophy in satellite cell-depleted skeletal muscle. *Development* **138**, 3657-3666. doi:10.1242/dev.068858

McLoon, L. K. and Wirtschafter, J. (2003). Activated satellite cells in extraocular muscles of normal adult monkeys and humans. *Invest. Ophthalmol. Vis. Sci.* **44**, 1927-1932. doi:10.1167/iovs.02-0673

Michaud, J. L., Lapointe, F. and Le Douarin, N. M. (1997). The dorsoventral polarity of the presumptive limb is determined by signals produced by the somites and by the lateral somatopleure. *Development* **124**, 1453-1463. doi:10.1242/dev.124.8.1453

Mierzejewski, B., Archacka, K., Grabowska, I., Florkowska, A., Ciemerych, M. A. and Brzoska, E. (2020a). Human and mouse skeletal muscle stem and progenitor cells in health and disease. *Semin. Cell Dev. Biol.* **104**, 93-104. doi:10.1016/j.semcdb.2020.01.004

Mierzejewski, B., Grabowska, I., Jackowski, D., Irhashava, A., Michalska, Z., Stremińska, W., Jańczyk-Ilach, K., Ciemerych, M. A. and Brzoska, E. (2020b). Mouse CD146+ muscle interstitial progenitor cells differ from satellite cells and present myogenic potential. *Stem Cell Res. Ther.* **11**, 341. doi:10.1186/s13287-020-01827-z

Mitchell, K. J., Pannérec, A., Cadot, B., Parlakian, A., Besson, V., Gomes, E. R., Marazzi, G. and Sassoon, D. A. (2010). Identification and characterization of a non-satellite cell muscle resident progenitor during postnatal development. *Nat. Cell Biol.* **12**, 257-266. doi:10.1038/ncb2025

Murach, K. A., Vechetti, I. J., Van Pelt, D. W., Crow, S. E., Dungan, C. M., Figueiredo, V. C., Kosmac, K., Fu, X., Richards, C. I., Fry, C. S. et al. (2020). Fusion-independent satellite cell communication to muscle fibers during load-induced hypertrophy. *Function (Oxf)* **1**, zqaa009. doi:10.1093/function/zqaa009

Murphy, M. M., Lawson, J. A., Mathew, S. J., Hutcheson, D. A. and Kardon, G. (2011). Satellite cells, connective tissue fibroblasts and their interactions are crucial for muscle regeneration. *Development* **138**, 3625-3637. doi:10.1242/dev.064162

Nassari, S., Duprez, D. and Fournier-Thibault, C. (2017). Non-myogenic contribution to muscle development and homeostasis: the role of connective tissues. *Front. Cell Dev. Biol.* **5**, 22. doi:10.3389/fcell.2017.00022

Nelson, L. T., Rakshit, S., Sun, H. and Wellik, D. M. (2008). Generation and expression of a Hoxa11eGFP targeted allele in mice. *Dev. Dyn.* **237**, 3410-3416. doi:10.1002/dvdy.21756

Pawlikowski, B., Pulliam, C., Betta, N. D., Kardon, G. and Olwin, B. B. (2015). Pervasive satellite cell contribution to uninjured adult muscle fibers. *Skelet. Muscle* **5**, 42. doi:10.1186/s13395-015-0067-1

Pineault, K. M., Song, J. Y., Kozloff, K. M., Lucas, D. and Wellik, D. M. (2019). Hox11 expressing regional skeletal stem cells are progenitors for osteoblasts, chondrocytes and adipocytes throughout life. *Nat. Commun.* **10**, 3168. doi:10.1038/s41467-019-11100-4

Qu-Petersen, Z., Deasy, B., Jankowski, R., Ikezawa, M., Cummins, J., Pruchnic, R., Mytinger, J., Cao, B., Gates, C., Wernig, A. et al. (2002). Identification of a novel population of muscle stem cells in mice: potential for muscle regeneration. *J. Cell Biol.* **157**, 851-864. doi:10.1083/jcb.200108150

Rivers, L. E., Young, K. M., Rizzi, M., Jamen, F., Psachoulia, K., Wade, A., Kessaris, N. and Richardson, W. D. (2008). PDGFRA/NG2 glia generate myelinating oligodendrocytes and piriform projection neurons in adult mice. *Nat. Neurosci.* **11**, 1392-1401. doi:10.1038/nn.2220

Rux, D. R., Song, J. Y., Swinehart, I. T., Pineault, K. M., Schlientz, A. J., Trulik, K. G., Goldstein, S. A., Kozloff, K. M., Lucas, D. and Wellik, D. M. (2016). Regionally restricted Hox function in adult bone marrow multipotent mesenchymal stem/stromal cells. *Dev. Cell* **39**, 653-666. doi:10.1016/j.devcel.2016.11.008

Sambasivan, R., Yao, R., Kissenpfennig, A., Van Wittenberghe, L., Paldi, A., Gayraud-Morel, B., Guenou, H., Malissen, B., Tajbakhsh, S. and Galy, A. (2011). Pax7-expressing satellite cells are indispensable for adult skeletal muscle regeneration. *Development* **138**, 3647-3656. doi:10.1242/dev.067587

Sefton, E. M. and Kardon, G. (2019). Connecting muscle development, birth defects, and evolution: an essential role for muscle connective tissue. *Curr. Top. Dev. Biol.* **132**, 137-176. doi:10.1016/bs.ctdb.2018.12.004

Swinehart, I. T., Schlientz, A. J., Quintanilla, C. A., Mortlock, D. P. and Wellik, D. M. (2013). Hox11 genes are required for regional patterning and integration of muscle, tendon and bone. *Development* **140**, 4574-4582. doi:10.1242/dev.096693

Tatsumi, R., Sankoda, Y., Anderson, J. E., Sato, Y., Mizunoya, W., Shimizu, N., Suzuki, T., Yamada, M., Rhoads, R. P., Ikeuchi, Y. et al. (2009). Possible implication of satellite cells in regenerative motoneuritogenesis: HGF upregulates neural chemorepellent Sema3A during myogenic differentiation. *Am. J. Physiol. Cell Physiol.* **297**, C238-C252. doi:10.1152/ajpcell.00161.2009

Tedesco, F. S., Moyle, L. A. and Perdiguero, E. (2017). Muscle interstitial cells: a brief field guide to non-satellite cell populations in skeletal muscle. *Methods Mol. Biol.* **1556**, 129-147. doi:10.1007/978-1-4939-6771-1_7

Thomas, K., Engler, A. J. and Meyer, G. A. (2015). Extracellular matrix regulation in the muscle satellite cell niche. *Connect. Tissue Res.* **56**, 1-8. doi:10.3109/03008207.2014.947369

Tidball, J. G. and Villalta, S. A. (2010). Regulatory interactions between muscle and the immune system during muscle regeneration. *Am. J. Physiol. Regul. Integr. Comp. Physiol.* **298**, R1173-R1187. doi:10.1152/ajpregu.00735.2009

Tramontano, A. F., O'Leary, J., Black, A. D., Muniyappa, R., Cutaia, M. V. and El-Sherif, N. (2004). Statin decreases endothelial microparticle release from human coronary artery endothelial cells: implication for the Rho-kinase pathway. *Biochem. Biophys. Res. Commun.* **320**, 34-38. doi:10.1016/j.bbrc.2004.05.127

Uezumi, A., Fukada, S.-I., Yamamoto, N., Takeda, S. and Tsuchida, K. (2010). Mesenchymal progenitors distinct from satellite cells contribute to ectopic fat cell formation in skeletal muscle. *Nat. Cell Biol.* **12**, 143-152. doi:10.1038/ncb2014

Uezumi, A., Ito, T., Morikawa, D., Shimizu, N., Yoneda, T., Segawa, M., Yamaguchi, M., Ogawa, R., Matev, M. M., Miyagoe-Suzuki, Y. et al. (2011). Fibrosis and adipogenesis originate from a common mesenchymal progenitor in skeletal muscle. *J. Cell Sci.* **124**, 3654-3664. doi:10.1242/jcs.086629

Watanabe, K., Ueno, M., Kamiya, D., Nishiyama, A., Matsumura, M., Wataya, T., Takahashi, J. B., Nishikawa, S.-I., Muguruma, K. and Sasai, Y. (2007). A ROCK inhibitor permits survival of dissociated human embryonic stem cells. *Nat. Biotechnol.* **25**, 681-686. doi:10.1038/nbt1310

Wellik, D. M. and Capecchi, M. R. (2003). Hox10 and Hox11 genes are required to globally pattern the mammalian skeleton. *Science* **301**, 363-367. doi:10.1126/science.1085672

White, R. B., Biérinx, A.-S., Gnocchi, V. F. and Zammit, P. S. (2010). Dynamics of muscle fibre growth during postnatal mouse development. *BMC Dev. Biol.* **10**, 21. doi:10.1186/1471-213X-10-21

Yin, H., Price, F. and Rudnicki, M. A. (2013). Satellite cells and the muscle stem cell niche. *Physiol. Rev.* **93**, 23-67. doi:10.1152/physrev.00043.2011

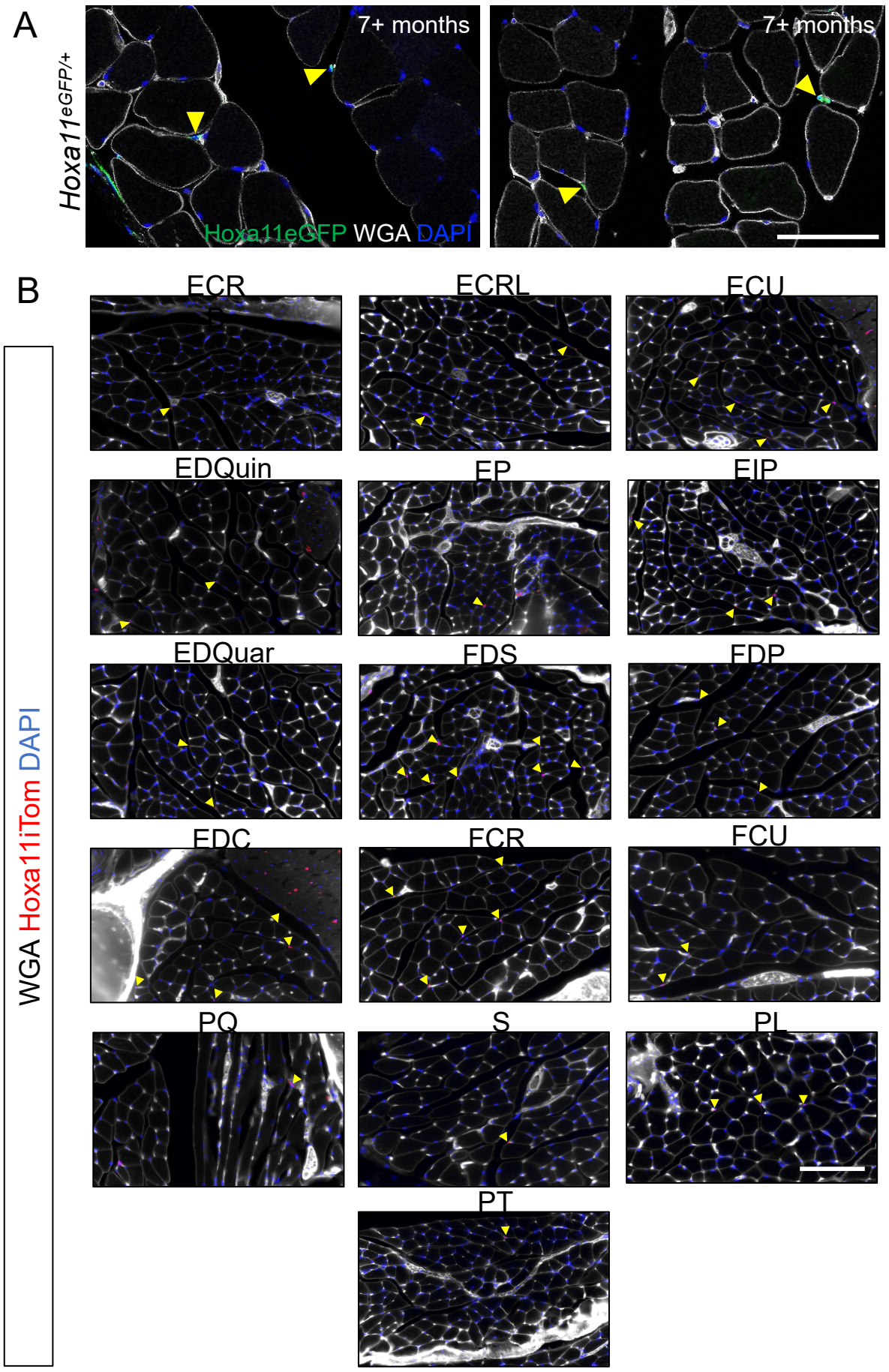

Figure S1. Hoxa11 expression in muscle interstitial cells is observed in aged mice and Hoxa11 lineage labeling of interstitial cells is observed in all forelimb muscles. (**A**) High magnification confocal microscopy shows Hoxa11eGFP-positive cells (green, yellow arrowheads) are observed in the muscle interstitium, defined by WGA, in animals 7 month of age - 1year old. Scale bar = 75 μm; N = 3 animals. (**B**) Expression of Hoxa11 in interstitial cells of individual forelimb muscles collected from *Hoxa11*$^{CreERT2/+}$ *; ROSA*$^{LSL\text{-}tdTomato/+}$ animals 3 days after tamoxifen treatment. High magnification images of Extensor Carpi Radialis Brevis (ECRB), Extensor Carpi Radialis Longus (ECRL), Extensor Carpi Ulnaris (ECU), Extensor Digiti Quinti (EDQuin), Extensor Pollicis (EP), Extensor Indicis Proprius (EIP), Extensor Digiti Quarti (EDQuar), Flexor Digitorum Sublimis (FDS), Flexor Digitorum Profundus (FDP), Extensor Digitorum Communis (EDC), Flexor Carpi Radialis (FCR), Flexor Carpi Ulnaris (FCU), Pronator Quadratus (PQ), Supinator (S), Palmaris Longus (PL), and Pronator Teres (PT). Scale bar = 100 μm; N = 4 animals.

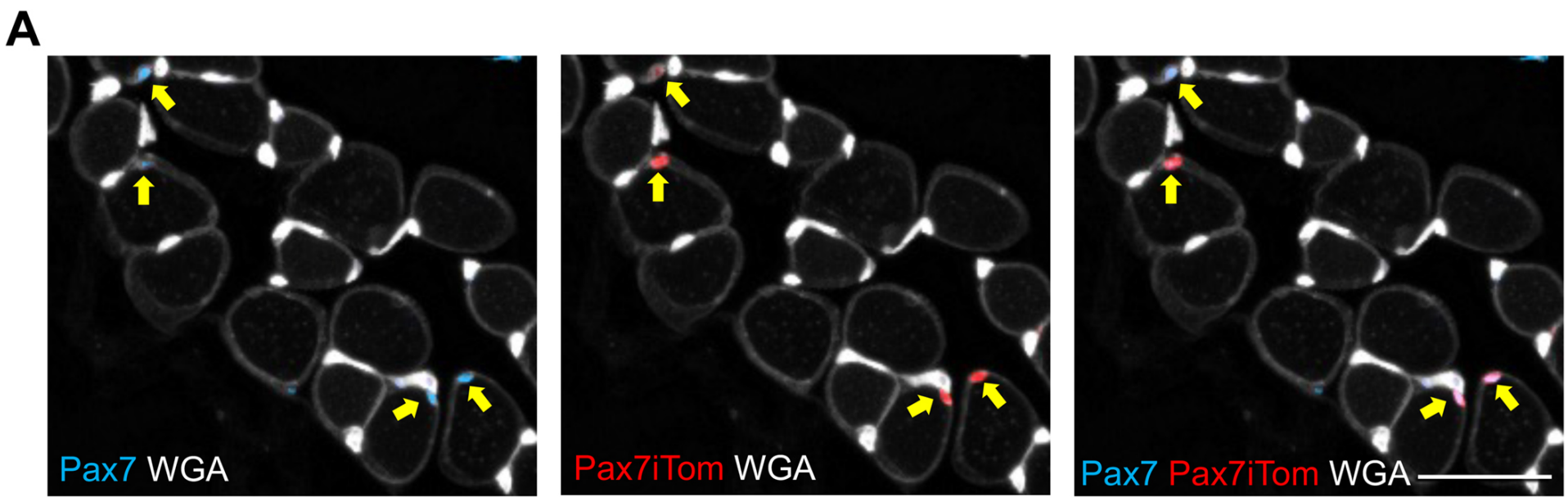

Fig. S2. Both *Hoxa11-CreERT2* and *Pax7-CreERT2* show approximately 90% efficiency with lineage reporter ROSA-LSL-tdTomato. (A) Images show Pax7 IF staining (blue) overlaps with tdTomato (red) in Pax7 lineage reporter animals (Pax7iTom) 4 days after tamoxifen treatment. Scale Bar = 50 μm. **(B)** Quantification of Pax7-CreERT2 efficiency was assessed by counting the number of Pax7 antibody-stained cells and tdTomato labeled cells at 48hrs (n= 2 animals) and 4 days (n= 2 animals) after Tamoxifen treatment. **(C)** Quantification of Hoxa11-CreERT2-induced recombination of ROSA-LSL-tdTomato with a single 5mg bolus of tamoxifen was assessed by counting the number of Hoxa11eGFP and tdTomato labeled cells at 48hrs (n=2 animals) and 7 days (n=2 animals) after tamoxifen administration. Both Cres resulted in approximately 90% efficiency.

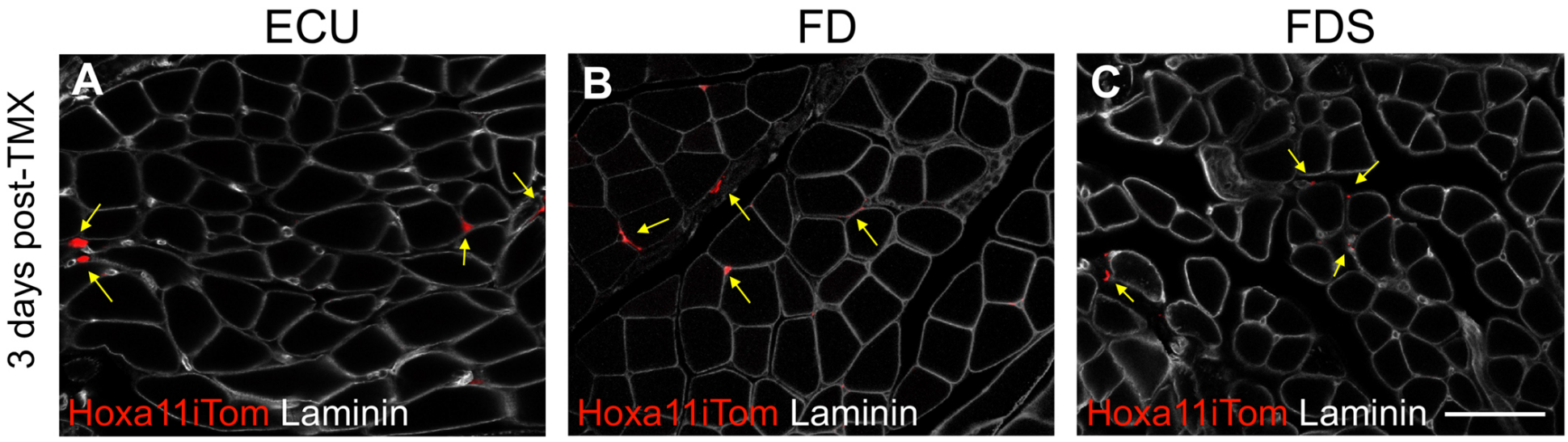

Fig. S3. Hoxa11 expressing cells are only in the interstitium of zeugopod-attached muscles after initial recombination. Hoxa11 lineage labeling (Hoxa11iTom, red) is observed 3 days following tamoxifen administration. (**A-C**) Hoxa11 lineage-labeled cells are only seen in the interstitium (yellow arrows) of the Extensor Carpi Ulnaris (ECU), Flexor Digitorum Profundus (FDP) and Flexor Digitorum Sublimis (FDS) as shown by laminin (white). Scale bar = 100 μm. N = 4 animals.

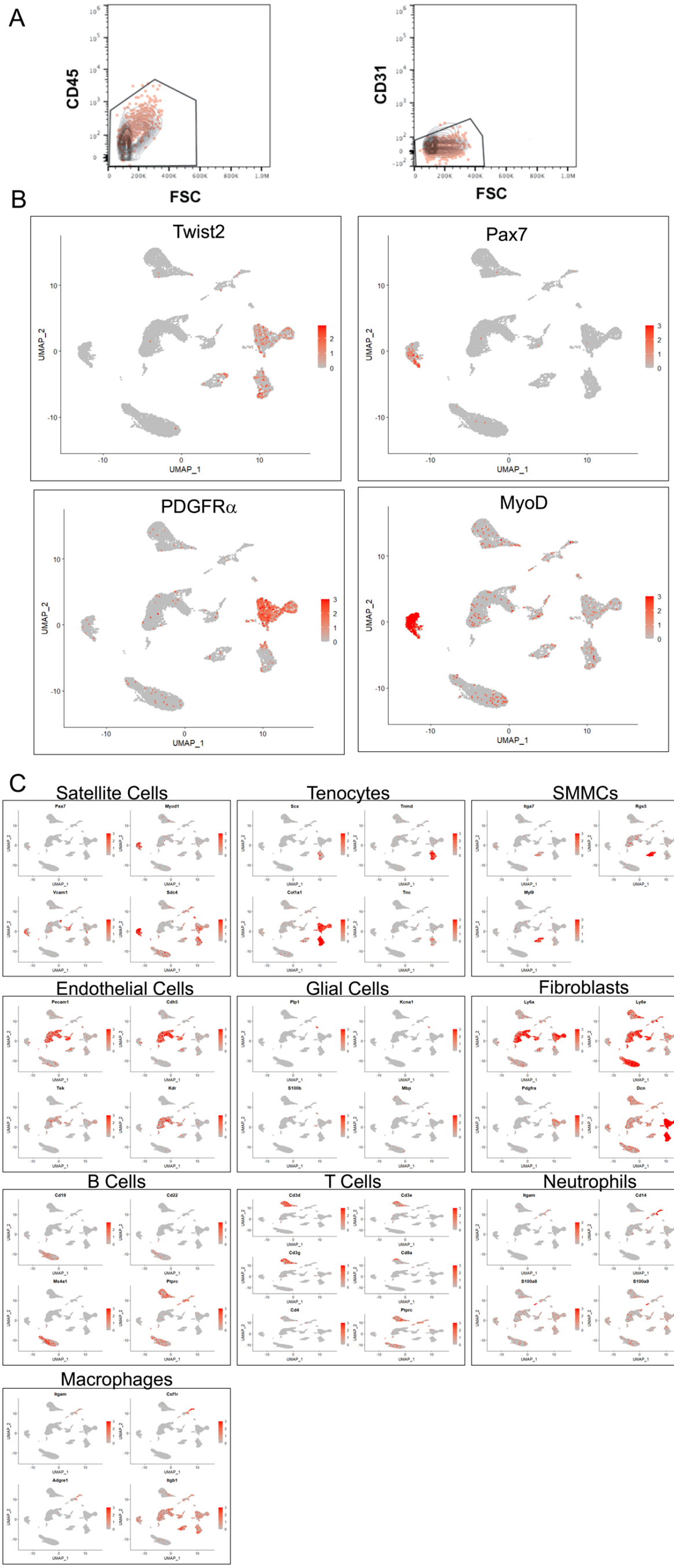

Fig. S4. Further flow cytometry and Sing-cell RNA-sequencing analyses. (A) Hoxa11iTom+ cells dotted (red) over contour plot of non-tdTom cells. The mononuclear subsets analyzed by flow cytometry were first gated to exclude hematopoietic and endothelial cells; Hoxa11iTom+ cells are non-hematopoietic and no-endothelial. **(B)** Plotting single gene expressions onto a UMAP projection show Twist2 and PDGFRα predominantly in fibroblasts, and Pax7 and MyoD predominantly found in satellite cells though low representations of each of these four genes are found in other clusters, highlighting the imprecision of statistical clustering with limited representation of expressed gene sets that is characteristic of single cell sequencing. **(C)** Additional feature plots for additional markers used to define subsets.

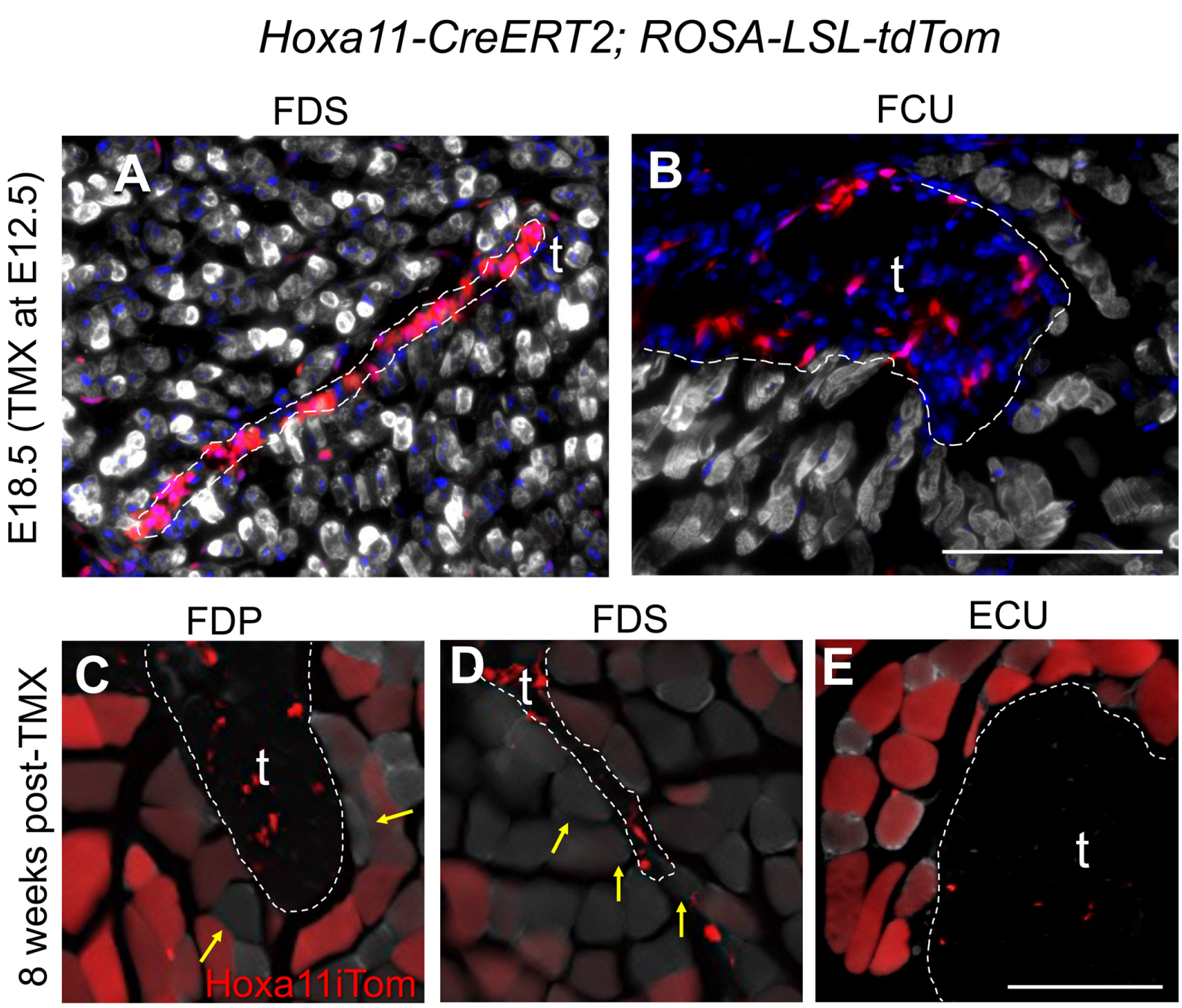

Fig. S5. Hoxa11 lineage shows no preferential contribution to myofibers near the myotendinous junctions during embryogenesis or homeostasis. (A,B) Sections of embryonic forelimb muscles were analyzed for myofiber lineage contribution at E18.5. N = 3 animals. **(C-E)** Images of the Flexor Digitorum Sublimis (FDS) and Flexor Carpi Ulnaris (FCU) muscles at the myotendinous junction show no Hoxa11iTom (red) overlap with My32 (white), consistent with lineage labeling throughout the rest of the muscle body. Sections from adult Hoxa11iTom muscle of the Flexor Digitorum Profundus (FDP), Flexor Digitorum Sublimis (FDS), and Extensor Carpi Ulnaris were analyzed for Hox11 lineage contribution at the myotendinous junction 8 weeks after the induction of lineage reporting. High magnification images show similar lineage labeling near the myotendinous junction of the FDP **(C)**, FDS **(D)**, or ECU **(E)** as in the mid-body of the muscle (Figure 4). N = 5 animals. Scale bars = 100 μm. Tendons are outlined with dashed line and marked by t.

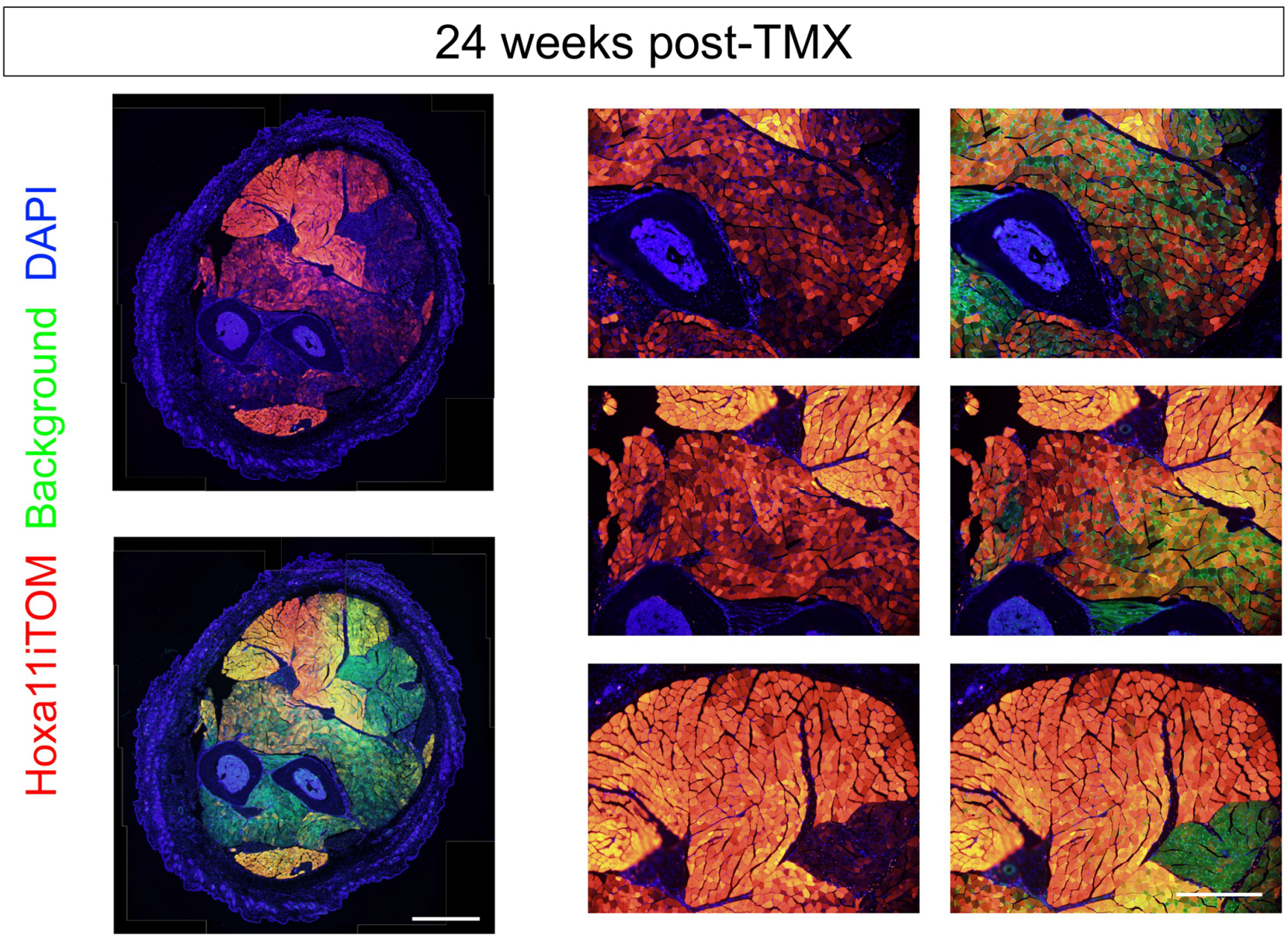

Fig. S6. Hoxa11 lineage 24 weeks after reporter induction. Hoxa11$^{CreERT2/+}$; ROSA$^{LSL\text{-}tdTomato/+}$ mice were given 5mg tamoxifen at 8 weeks of age and collected 24 weeks (6 months) later. A full cross-section with and without background (green) show many Hoxa11iTom^{+} (red) muscle fibers. Close-ups with and without background depict high levels of tdTomato within muscle fibers. Scale bars = 1000 μm and 500 μm, respectively. N = 2 animals.

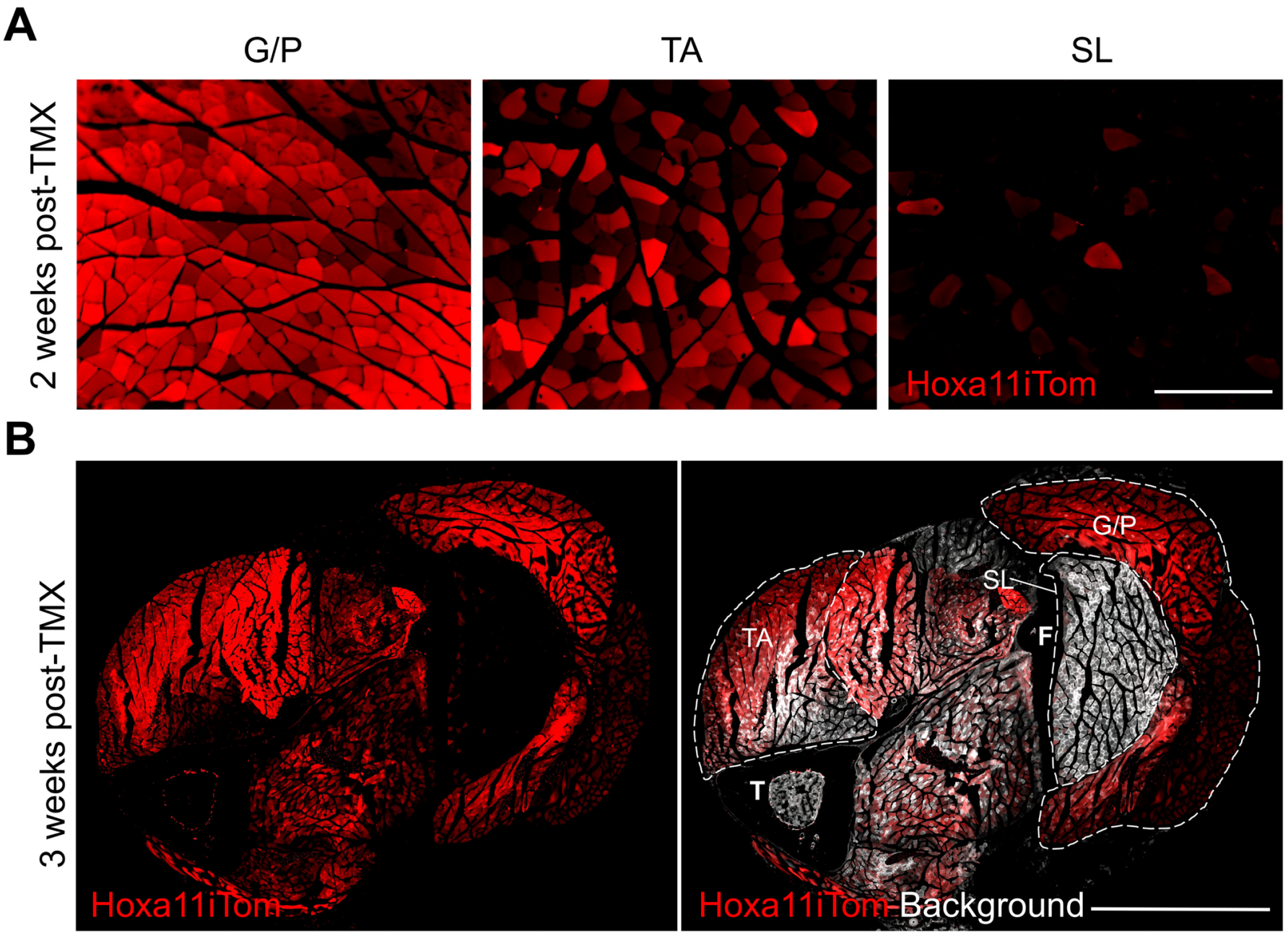

Fig. S7. Hoxa11 lineage differentially contributes to hindlimb muscles. (A) Hindlimb muscles taken from Hoxa11iTom animals 2 weeks after tamoxifen treatment show different levels of lineage contribution in the Gastrocnemius/Plantaris (G/P), Tibialis Anterior (TA), and Soleus (SL). Scale bar = 200 μm. N = 4 animals. **(B)** A whole hindlimb cross-section from an animal 3 weeks after the start of lineage labeling shows variable tdTom expression in muscles of the hindlimb. T and F mark the tibia and fibula, respectively. Scale bar = 1000 μm. N = 1 animal. Muscles shown in **A** are outlined and labeled in **B**.

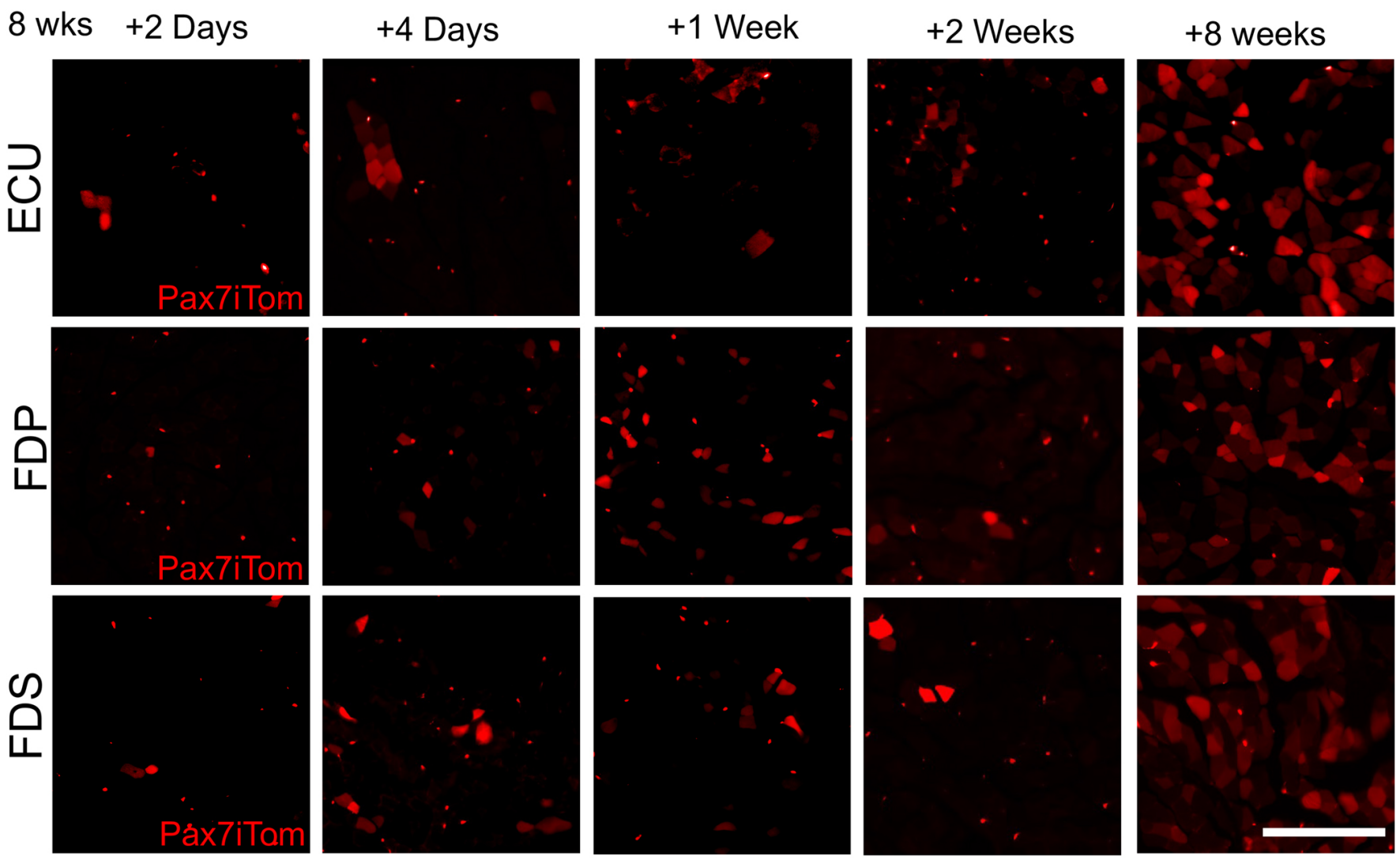

Fig. S8. Pax7iTom lineage in the forelimb muscles. *Pax7CreERT2; ROSALSL-TdTomato* (Pax7iTom) mice were given a single intraperitoneal injection of 5 mg tamoxifen at 8 weeks of age and collected at 2 days, 4 days, 1 week, 2 weeks, and 8 weeks after tamoxifen induction. Images of the Extensor Carpi Ulnaris (ECU), Flexor Digitorum Profundus (FDP) and Flexor Digitorum Sublimis (FDS) muscles show tdtom+ myofibers as well as tdTom+ satellite cells. N = 3 (2d, 4d, 7d, 2wk) and 4 (8wk) animals per timepoint. Scale bar = 200 μm.

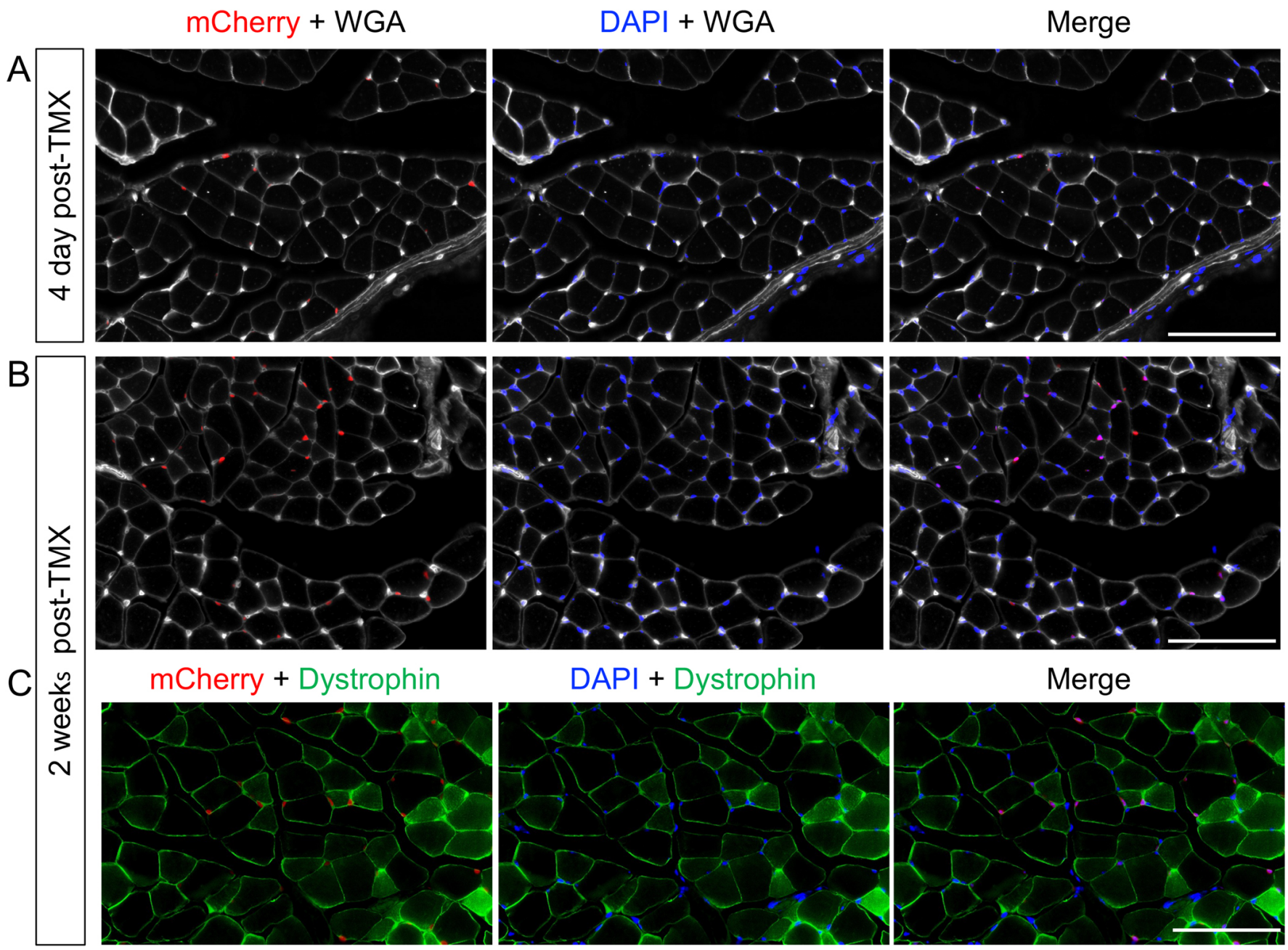

Fig. S9. Hoxa11iH2BmCherry-labeled nuclei overlap with nuclear stain. H2BmCherry expression in nuclei shown in Fig. 5 was confirmed with DAPI nuclear stain in images 4 days (**A**), 2 weeks (**B**) post tamoxifen, and dystrophin stain (**C**). Muscle fiber outer membranes were stained with WGA (**A,B**). Scale bars = 100 μm. N = 3 animals (4 day) and 2 animals (2 weeks).

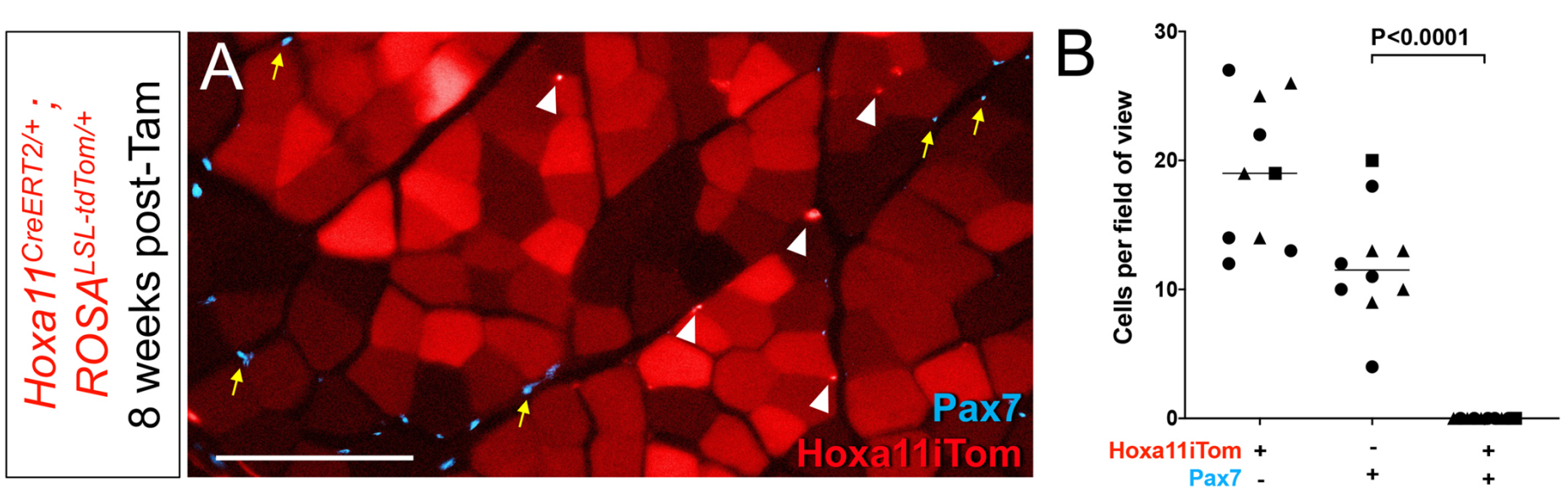

Fig. S10. Hoxa11 lineage does not label satellite cells 8 weeks post-induction of lineage reporter. (**A**) Forelimb muscle sections from animals 8 weeks (dosing at 8 weeks of age, collection at 16 weeks of age) after the start of lineage labeling were stained for Pax7 (cyan, yellow arrows) and analyzed for overlap of Hoxa11itom (red, arrowheads) and Pax7. (**B**) Quantification shows no Hoxa11iTom+/ Pax7+ cells were observed through forelimb muscles. Scale bar = 100 μm. N = 3 animals.

Table S1. Antibodies

Name	Source	Catalog Number	Dilution	Antigen retrival
anti-GFP	Aves Labs	GFP-1010	1:200	No
anti-Twist2	Abcam	ab66031	1:200	No
anti-PDGFRa	Abcam	ab61219	1:50	No
anti-Tcf4	Cell Signaling	2569S	1:100	No
WGA-647	Invitrogen	W32466	1:250	No
WGA-488	Invitrogen	W11261	1:250	No
anti-Pax7	DSHB	Pax7-S	1:10	Yes
anti-Laminin	Sigma	L9393	1:500	No
anti-My32	Sigma	M4276	1:400	Yes
anti-PECAM1	DSHB	2H8-S	1:10	No
anti-BF-F3	DSHB	BF-F3	1:10	Yes
anti-SC-71	DSHB	SC-71	1:10	Yes
anti-Myosin (Skeletal, Slow)	Sigma	M8421	1:250	Yes
anti-ScaI(Ly6A/E)-BV711	Biolegend	108131	1:100	No
anti-CD34-PE-Cy7	Biolegend	119325	1:100	No
anti-CD31-PE-CF594	BD-Horizon	563616	1:100	No
anti-ITGA7-AF647	AbLab	67-0010-05	1:100	No
anti-CD45-FITC	Biolegend	304005	1:100	No
anti-CD106(VCAM1)-PE/Cy7	Biolegend	105719	1:40	No
Alexa-488 Donkey anti-Chicken	Jackson ImmunoResearch Labs	016-580-084	1:500	No
Alexa-555 Donkey anti-Rabbit	Invitrogen	A31572	1:500	No
Streptavidin-AF647	Invitrogen	S21374	1:500	No
Anti-Dystrophin	Thermofisher	PA1-21011	1:100	Yes